in NF-κB activation through lymphotoxin β receptor, but not through tumor necrosis factor receptor I. J. Exp. Med. **193**:631–636.
40. **Mattioli, I., A. Sebald, C. Bucher, R. P. Charles, H. Nakano, T. Doi, M. Kracht, and M. L. Schmitz.** 2004. Transient and selective NF-kappa B p65 serine 536 phosphorylation induced by T cell costimulation is mediated by I kappa B kinase β and controls the kinetics of p65 nuclear import. J. Immunol. **172**:6336–6344.
41. **Mercurio, F., H. Zhu, B. W. Murray, A. Shevchenko, B. L. Bennett, J. Li, D. B. Young, M. Barbosa, M. Mann, A. Manning, and A. Rao.** 1997. IKK-1 and IKK-2: cytokine-activated kinases essential for NF-κB activation. Science **278**:860–866.
42. **Murata, T., M. Shimada, S. Sakakibara, T. Yoshino, H. Kadono, T. Masuda, M. Shimazaki, T. Shintani, K. Fuchikami, K. Sakai, H. Inbe, K. Takeshita, T. Niki, M. Umeda, K. B. Bacon, K. B. Ziegelbauer, and T. B. Lowinger.** 2003. Discovery of novel and selective IKK-β serine-threonine protein kinase inhibitors. Part 1. Bioorg. Med. Chem. Lett. **13**:913–918.
43. **Murata, T., M. Shimada, S. Sakakibara, T. Yoshino, T. Masuda, T. Shintani, H. Sato, Y. Koriyama, K. Fukushima, N. Nunami, M. Yamauchi, K. Fuchikami, H. Komura, A. Watanabe, K. B. Ziegelbauer, K. B. Bacon, and T. B. Lowinger.** 2004. Synthesis and structure-activity relationships of novel IKK-β inhibitors. Part 3. Orally active anti-inflammatory agents. Bioorg. Med. Chem. Lett. **14**:4019–4022.
44. **Nabel, G., and D. Baltimore.** 1987. An inducible transcription factor activates expression of human immunodeficiency virus in T cells. Nature **326**: 711–713.
45. **Okamoto, H., T. P. Cujec, M. Okamoto, B. M. Peterlin, M. Baba, and T. Okamoto.** 2000. Inhibition of the RNA-dependent transactivation and replication of human immunodeficiency virus type 1 by a fluoroquinoline derivative K-37. Virology **272**:402–408.
46. **Okamoto, M., M. Ono, and M. Baba.** 1998. Potent inhibition of HIV type 1 replication by an anti-inflammatory alkaloid, cepharantine, in chronically infected monocytic cells. AIDS Res. Hum. Retrovir. **14**:1239–1245.
47. **Okamoto, T., and F. Wong-Staal.** 1986. Demonstration of virus-specific transcriptional activator(s) in cells infected with HTLV-III by an in vitro cell-free system. Cell **47**:29–35.
48. **Okamoto, T., S. Sakurada, J. P. Yang, and J. P. Merin.** 1997. Regulation of NF-κB and disease control: identification of a novel serine kinase and thioredoxin as effectors for signal transduction pathway for NF-κB activation. Curr. Top. Cell. Regul. **35**:149–161.
49. **Okamoto, T., T. Benter, S. F. Josephs, M. R. Sadie, and F. Wong-Staal.** 1990. Transcriptional activation from the long terminal repeat of human immunodeficiency virus in vitro. Virology **177**:606–614.
50. **Okamoto, T., T. Matsuyama, S. Mori, S. Hamamoto, N. Kobayashi, N. Yamamoto, S. F. Josephs, F. Wong-Staal, and K. Shimotohno.** 1989. Augmentation of human immunodeficiency virus type 1 gene expression by tumor necrosis factor-α. AIDS Res. Hum. Retrovir. **5**:131–138.
51. **Persaud, D., Y. Zhou, J. M. Siliciano, and R. F. Siliciano.** 2003. Latency in human immunodeficiency virus type 1 infection: no easy answers. J. Virol. **77**:1659–1665.
52. **Peterlin, B. M., and D. Trono.** 2003. Hide, shield and strike back: how human immunodeficiency virus-infected cells avoid immune eradication. Nat. Rev. Immunol. **3**:97–107.
53. **Pomerantz, R. J.** 2002. Reservoirs of human immunodeficiency virus type 1: the main obstacles to viral eradication. Clin. Infect. Dis. **34**:91–97.
54. **Quinto, I., M. Mallardo, F. Baldassarre, G. Scala, G. Englund, and K. T. Jeang.** 1999. Potent and stable attenuation of live-HIV-1 by gain of a proteolysis-resistant inhibitor of NF-κB (IκB-αS32/36A) and the implications for vaccine development. J. Biol. Chem. **274**:17567–17572.
55. **Roulston, A., R. Lin, P. Beauparlant, M. A. Wainberg, and J. Hiscott.** 1995. Regulation of HIV-1 and cytokine gene expression in myeloid cells by NF-κB/Rel transcription factors. Microbiol. Rev. **59**:481–505.
56. **Sakurai, H., S. Suzuki, N Kawasaki, H. Nakano, T. Okazaki, A. Chino, T. Doi, and I. Saiki.** 2003. Tumor necrosis factor-α-induced IKK phosphorylation of NF-κB p65 on serine 536 is mediated through the TRAF2, TRAF5, and TAK1 signaling pathway. J. Biol. Chem. **278**:36916–36923.
57. **Sanda, T., S. Iida, H. Ogura, K. Asamitsu, T. Murata, K. B. Bacon, R. Ueda, and T. Okamoto.** 2005. Growth inhibition of multiple myeloma cells by a novel IκB inhibitor. Clin. Cancer Res. **11**:1974–1982.
58. **Sarol, L. C., K. Imai, K. Asamitsu, T. Tetsuka, N. G. Barzaga, and T. Okamoto.** Inhibitory effects of IFN-γ on HIV-1 replication in latently infected cells. Biochem. Biophys. Res. Commun. **291**:890–896.
59. **Sato, T., K. Asamitsu, J. P. Yang, N. Takahashi, T. Tetsuka, A. Yoneyama, A. Kanagawa, and T. Okamoto.** 1998. Inhibition of human immunodeficiency virus type 1 replication by a bioavailable serine/threonine kinase inhibitor, fasudil hydrochloride. AIDS Res. Hum. Retrovir. **14**:293–298.
60. **Senftleben, U., Y. Cao, G. Xiao, F. R. Greten, G. Krahn, G. Bonizzi, Y. Chen, Y. Hu, A. Fong, S. C. Sun, and M. Karin.** 2001. Activation of IKK-α of a second, evolutionary conserved, NF-κB signaling pathway. Science **293**:1495–1499.
61. **Sun, S. C., P. A. Ganchi, D. W. Ballard, and W. C. Greene.** 1993. NF-κB controls expression of inhibitor IκBα: Evidence for an inducible autoregulatory pathway. Science **259**:1912–1915.
62. **Takeda, K., O. Takeuchi, T. Tsujimura, S. Itami, O. Adachi, T. Kawai, H. Sanjo, K. Yoshikawa, N. Terada, and S. Akira.** 1999. Limb and skin abnormalities in mice lacking IKK-α. Science **284**:313–316.
63. **Teranishi, F., Z.-Q. Liu, M. Kunimatsu, K. Imai, H. Takeyama, T. Manabe, M. Sasaki, and T. Okamoto.** 2003. Calpain is involved in the HIV replication from the latently infected OM10.1 cells. Biochem. Biophys. Res. Commun. **303**:940–946.
64. **Traber, K. E., H. Okamoto, C. Kurono, M. Baba, C. Saliou, T. Soji, L. Packer, and T. Okamoto.** 1999. Anti-rheumatic compound aurothioglucose inhibits tumor necrosis factor-α-induced HIV-1 replication in latently infected OM10.1 and Ach2 cells. Int. Immunol. **11**:143–150.
65. **Viatour, P., M. P. Merville, V. Bours, and A. Chariot.** 2005. Phosphorylation of NF-κB and IκB proteins: implications in cancer and inflammation. Trends Biochem. Sci. **30**:43–52.
66. **Wang, D., and A. S. Baldwin.** 1998. Activation of nuclear factor-κB-dependent transcription by tumor necrosis factor-α is mediated through phosphorylation of RelA/p65 on Serine 529. J. Biol. Chem. **273**:29411–29416.
67. **West, M. J., A. D. Lowe, and J. Karn.** 2001. Activation of human immunodeficiency virus transcription in T cells revisited: NF-κB p65 stimulates transcriptional elongation. J. Virol. **75**:8524–8537.
68. **Xiao, G., E. W. Harhaj, and S. C. Sun.** 2001. NF-κB-inducing kinase regulates processing of NF-κB2 p100. Mol. Cell **7**:401–409.
69. **Yamamoto, Y., and R. B. Gaynor.** 2004. IκB kinases: key regulators of the NF-κB pathway. Trends Biochem. Sci. **29**:72–79.
70. **Yamamoto, Y., U. N. Verma, S. Prajapati, Y. T. Kwak, and R. B. Gaynor.** 2003. Histone H3 phosphorylation by IKK-α is critical for cytokine induced gene expression. Nature **423**:655–659.
71. **Zandi, E., D. M. Rothwarf, M. Delhase, M. Hayakawa, and M. Karin.** 1997. The IκB kinase complex (IKK) contains two kinase subunits, IKKα and IKKβ, necessary for IκB phosphorylation and NF-κB activation. Cell **991**: 243–252.
72. **Zhong, H., H. SuYang, H. Erdjument-Bromage, P. Tempst, and S. Ghosh.** 1997. The transcriptional activity of NF-κB is regulated by the IκB-associated PKAc subunit through a cyclic AMP-independent mechanism. Cell **89**:413–124.

53BP2 induces apoptosis through the mitochondrial death pathway

Shinya Kobayashi[1,2,†], Shinichi Kajino[1,2,†], Naoko Takahashi[1], Satoshi Kanazawa[1], Kenichi Imai[1], Yurina Hibi[1], Hirotaka Ohara[2], Makoto Itoh[2] and Takashi Okamoto[1,*]

[1]*Department of Molecular and Cellular Biology, and* [2]*Department of Internal Medicine and Bioregulation, Nagoya City University Graduate School of Medical Sciences, 1 Kawasumi, Mizuho-cho, Mizuho-ku, Nagoya, Aichi 467-8601, Japan*

The p53 binding protein 2 (53BP2) has been identified as the interacting protein to p53, Bcl-2, and p65 subunit of nuclear factor κB (NF-κB). The TP53BP2 gene encodes two splicing variants, 53BP2S and 53BP2L, previously known as apoptosis stimulating protein 2 of p53 (ASPP2). We found that these 53BP2 proteins are located predominantly in the cytoplasm and induce apoptosis as demonstrated by cleavage of poly ADP ribose polymerase (PARP) and annexinV staining. Furthermore, we demonstrate that 53BP2 is located in the mitochondria and induces apoptosis associated with depression of the mitochondrial trans-membrane potential ($\Delta\Psi m$) and activation of caspase-9. From these findings we conclude that 53BP2 induces apoptosis through the mitochondrial death pathway.

Introduction

Apoptosis is a well-defined biochemical pathway and is essential for the maintenance of cellular homeostasis in metazoans. Accumulating evidences indicate that the normal apoptotic pathway is affected in the pathological processes such as cancer and autoimmunity (Fisher *et al.* 1995; Green & Reed 1998; Jackson & Puck 1999; Daniel & Korsmeyer 2004). The induction of apoptosis occurs through two distinct pathways, the one elicited by death receptors in the plasma membrane ('extrinsic pathway') and the other directly involving mitochondria ('intrinsic pathway'). Whereas the former primarily involves activation of caspase-8, the latter apoptosis pathway is associated with the release of cytochrome C from mitochondria and activation of caspase-9 (for a review see Judith *et al.* 2004).

The p53 binding protein 2 (53BP2) has been initially identified as an interacting protein to p53 (Iwabuchi *et al.* 1994) and implicated in the biological action of p53. It was also shown that the 53BP2 binding site in the p53 core domain is evolutionarily conserved and is frequently mutated in human cancer (Iwabuchi *et al.* 1994; Gorina & Pavletich 1996). The subsequent studies have revealed that it interacts with Bcl-2 (Naumovski & Cleary 1996) and p65 subunit of nuclear factor κB (NF-κB) (Yang *et al.* 1999). Interestingly, 53BP2 has been shown to induce apoptosis (Yang *et al.* 1999), which was confirmed by others (Lopez *et al.* 2000; Ao *et al.* 2001; Samuels-Lev *et al.* 2001; Bergamaschi *et al.* 2004). However, the mechanism by which 53BP2 induces apoptosis has not been clarified.

53BP2 protein is encoded by a single copy gene *TP53BP2* located in the long arm of chromosome 1 at q42.1 (Yang *et al.* 1997). We have recently found that it encodes two distinct mRNA species, either with or without exon 3, by alternative splicing (Takahashi *et al.* 2004) (Fig. 1A). These splicing variants encode two 53BP2 proteins containing 1005 and 1128 amino acids (aa) with the longer isoform containing additional 123 amino acids in the N-terminus where no known functional motif or distinct intracellular localization signal is found. Although Samuels-Lev *et al.* (2001) renamed the longer 53BP2 isoform as ASPP2 (apoptosis stimulating protein of p53 2), we have proposed to call these proteins as 53BP2S (short) and 53BP2L (long) based on the genome organization of *TP53BP2* transcripts (Takahashi *et al.* 2004). 53BP2 proteins contain several structural and functional motifs including Gln-rich α-helical region, Pro-rich regions, ankyrin repeats, and Src-homology 3 domain.

Communicated by: Masayuki M. Yamamoto
**Correspondence*: E-mail: tokamoto@med.nagoya-cu.ac.jp
[†]These two authors contributed equally to this work.

DOI: 10.1111/j.1365-2443.2005.00835.x

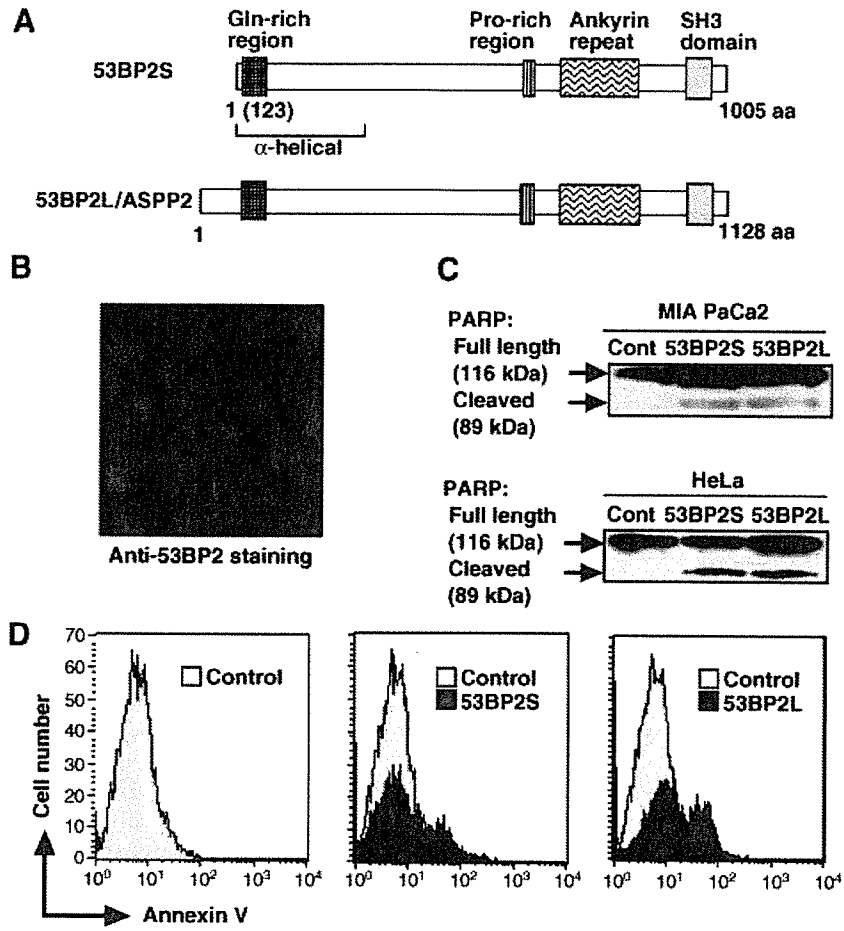

Figure 1 Induction of apoptosis by 53BP2 proteins. (A) Diagrammatic representation of 53BP2S and 53BP2L/ASPP2 proteins. Locations of Gln-rich region, putative 'α-helical region,' Pro-rich region, ankyrin repeats, and SH3 domain are indicated. Two splicing variants, 53BP2S and 53BP2L/ASPP2, containing 1005 amino acids and 1128 amino acids residues, respectively, are encoded by the same gene *TP53BP2* (Takahashi *et al.* 2004). 53BP2L contains additional 123 amino acid N-terminal region containing no apparent functional/structural motifs. (B) The localization of endogenous 53BP2 proteins in MIA PaCa-2 cells. Subcellular localization of endogenous 53BP2 was examined by immunostaining with anti-53BP2 mouse monoclonal antibody. The dim staining of 53BP2 proteins was repeatedly observed, which is presumably due to the low protein stability as previously indicated (Yang *et al.* 1999; Lopez *et al.* 2000). (C) Cleavage of PARP by 53BP2 proteins. MIA PaCa-2 cells and HeLa cells were transfected with pcDNA3.1–53BP2 ('53BP2S') or pCEP4-ASPP2 ('53BP2L') plasmids and the cell lysates were immunoblotted with anti-PARP antibody. The intact form of PARP (116 kDa) and its cleavage form (89 kDa) were detected by an anti-PARP rabbit polyclonal antibody (indicated by arrows). Note that no significant difference of the amounts of the cleaved form of PARP was found in cells expressing 53BP2S and 53BP2L. Cont, cells transfected with a control expression vector pcDNA3.1. (D) Induction of apoptosis by over-expression of 53BP2 proteins. MIA PaCa-2 cells were transfected with pcDNA3.1–53BP2 or pCEP4-ASPP2 and cells undergoing apoptosis were detected by flow cytometry. Live and dead cells were discriminated on the basis of their forward and side light-scattering properties. In order to evaluate cells undergoing apoptosis, cells were stained by both annexinV-PE and 7-AAD and those cells expressing 7-AAD were excluded from the measurement. The transfection efficiency was estimated to be approximately 65% by the GFP expression from the co-transfected pEGFP plasmid. The experiments were repeated more than three times with the same results.

In this study, we demonstrate that two 53BP2 isoforms, 53BP2S (previously called '53BP2') and 53BP2L ('ASPP2'), are localized predominantly in the cytoplasm and similarly induce apoptosis. We found that the mitochondrial death pathway is involved in the 53BP2-mediated apoptosis. The biological roles of 53BP2 and its interacting proteins in the regulation of apoptosis are discussed.

Results

Induction of apoptosis by 53BP2 proteins

Figure 1A illustrates the organization of 53BP2 isoforms as previously reported (Takahashi *et al.* 2004). As shown in Fig. 1B, the endogenous 53BP2 proteins were localized predominantly in the cytoplasm, confirming the previous reports wherein 53BP2 was over-expressed (Iwabuchi *et al.* 1998; Yang *et al.* 1999). To compare the effect of 53BP2S and 53BP2L, these proteins were transduced in MIA PaCa-2 and HeLa cells. After 48 h of transfection, the cleaved form of poly ADP ribose polymerase (PARP; 89 kDa product), a hallmark of apoptosis, was detected (Fig. 1C). When 53BP2S and 53BP2L were over-expressed in MIA PaCa-2 cells, approximately 16% and 27% of cells were found undergoing early apoptotic process (annexin V (+), 7-AAD (–)), respectively, whereas the percentage of apoptotic cells in the control was only 1.8% (Fig. 1D). The extents of apoptosis were similar to our previous observations using various DNA damaging agents (Mori *et al.* 2000).

Induction of apoptosis in a stable transfectant (293/53BP2)

We then examined the action of 53BP2 using the 293/53BP2 cells, in which expression of 53BP2S is under stringent control by ponasteron A (pon A). In Fig. 2A, both 293/53BP2 and its control 293/LZ were treated with pon A. The 53BP2S protein became detectable after 12 h of induction by pon A (5 μM) in a time-dependent manner and induced apoptosis as early as 24 h after pon A treatment. As shown in Fig. 2B, after 72 h of 53BP2S expression, a significant number (26%) of cells underwent apoptosis as revealed by positive staining for annexin V, whereas only the background level (6.5%) was stained in control cells. Cells at early apoptotic process (annexin (+), 7-AAD (–)) were found 14% and 3% in 293/53BP2 cells and control cells, respectively (Fig. 2B). No cleavage of PARP or a significant annexin V staining was detected with the control 293/LZ cells (data not shown).

Cytosolic and mitochondrial localization of 53BP2S

In Fig. 3A, intracellular localization of 53BP2S was examined by transfection of pEGFP53BP2 expressing 53BP2S in fusion with green fluorescence protein (GFP). A punctate vesicular pattern was noted, localized predominantly in the cytoplasm of the transfected cells. To confirm the localization of 53BP2S, we co-transfected pDsRed2-Mito, expressing red fluorescent protein targeted to mitochondria. As demonstrated in Fig. 3A and

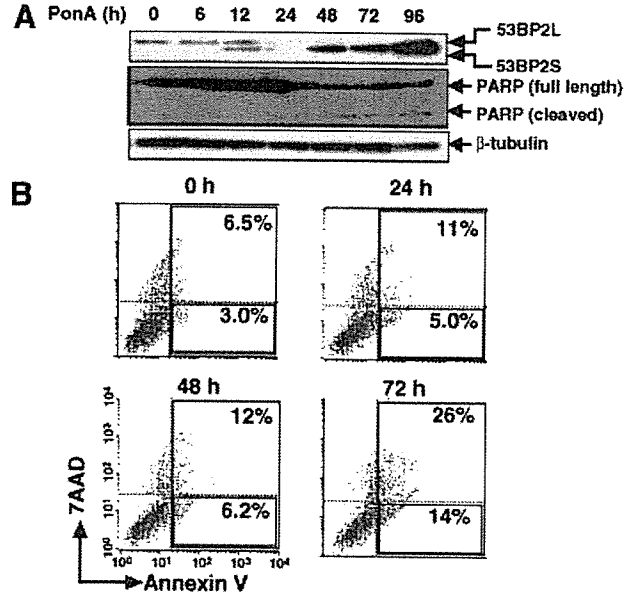

Figure 2 Induction of apoptosis in 293/53BP2 cell line. (A) Time course of induction of 53BP2S and cleavage of PARP in 293/53BP2 cells. Cells were treated with pon A (5 μM) using an ecdysone-inducible expression system for the indicated periods (h), and the cell lysate (10 μg protein) was examined for the expression of 53BP2S and PARP. The intact full-length PARP (116 kDa) was cleaved into 89 kDa during the apoptotic process. Longer exposure of chemiluminescence for protein detection revealed the endogenous 53BP2L protein in these cells. β-tubulin was used as an internal control. (B) Flow cytometric detection of apoptotic cells. 293/53BP2 cells were stimulated with pon A (5 μM) and cultured for the indicated periods (h). The percentages of cells at apoptosis (annexin V (+)) and cells at early apoptosis (annexin V positive and 7-AAD (–)) were counted and indicated separately.

53BP2S was shown to be partly localized in the mitochondria in addition to the cytoplasm. In most cells only portions of mitochondria were costained with 53BP2S, suggesting that small amounts of 53BP2S molecules could be sufficient to induce apoptosis. In Fig. 3B, subcellular fractionation was performed and the presence of 53BP2S was examined. Protein expression was induced by pon A for 48 h and each subcellular fraction was subjected to Western blotting with anti-53BP2 antibody. Although majority of the 53BP2S protein was detected in the cytosolic fraction, it was also detected in the mitochondrial fraction (Fig. 3B).

Depression of $\Delta\Psi$m by 53BP2S expression

These findings suggested the involvement of the 'intrinsic' death pathway. We thus examined the change in $\Delta\Psi$m

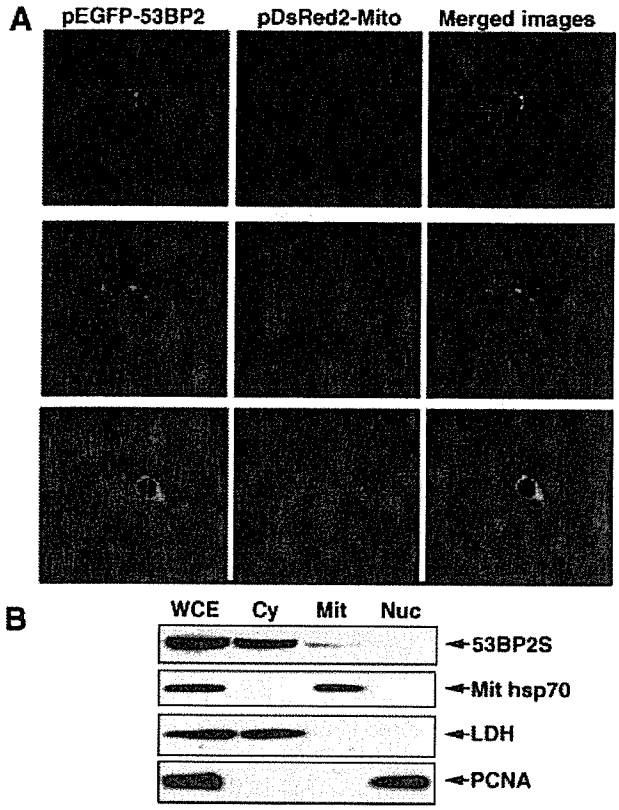

Figure 3 Intracellular localization of 53BP2S. (A) Co-localization of 53BPS and mitochondria marker. 293 cells were transiently transfected with pEGFP-53BP2 and mitochondria-targeting plasmid pDsRed2-Mit and examined under confocal microscope. The GFP fluorescence, DsRed fluorescence and merged images of cells are shown. Note that only portions of mitochondria (visualized by DsRed) were costained with GFP (53BP2S). (B) Subcellular fractionation. Upon induction of 53BP2 by pon A (5 μM, 48 h) in 293/53BP2 cells, whole cell extract (WCE) was prepared. The cytoplasmic (Cy), mitochondrial (Mit) and nuclear (Nuc) fractions were separated as described in Experimental procedures. Each protein fraction was separated by 10% SDS-PAGE, and probed with antibodies to 53BP2S, PCNA (nuclear marker), mitochondrial heat shock protein (Mit hsp70) and LDH (cytoplasmic marker). The same cell equivalents were loaded on each lane. Contamination of the cytoplasmic fraction into the mitochondria fraction was considered negligible because of the absence of LDH. The identical results were obtained repeatedly.

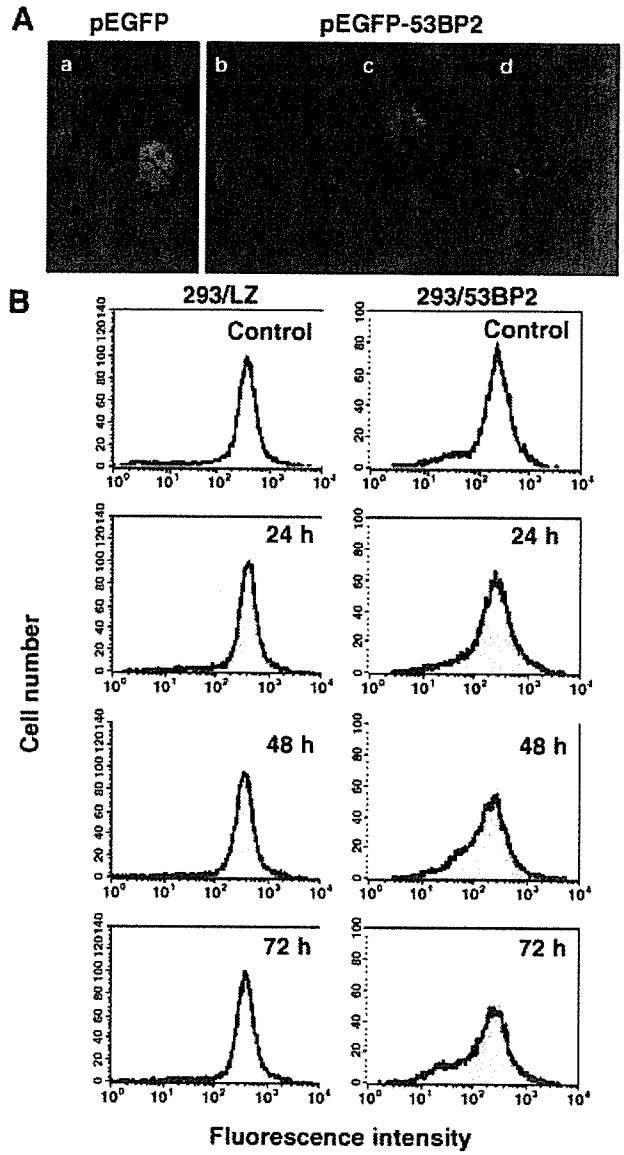

Figure 4 Alteration of the mitochondria transmembrane potential ($\Delta\Psi m$) by 53BP2S. (A) Reduction of $\Delta\Psi m$ by 53BP2S. After 48 h of transfection with pEGFP (a) or pEGFP53BP2 (b–d) plasmids, MIA PaCa-2 cells were stained with CMXRos. Typical cells are shown. In cells expressing 53BP2S, progressive reduction of $\Delta\Psi m$ was observed in association with nuclear fragmentation (from b–d). The same exposure time was used in each picture. (B) Temporal change of $\Delta\Psi m$ following 53BP2S induction. 293/53BP2 and 293/LZ cells were treated with pon A for indicated periods (h), stained with rhodamine 123, and flow cytometric analysis was performed. Distribution of fluorescence intensity of cells with sham treatment (only the solvent ethanol was added) is shown in gray shadow. 'Control,' uninduced cells.

following 53BP2S expression (Fig. 4). Several cationic, lipophilic, fluorescent dyes such as CMXRos and rhodamine 123, can readily detect changes in $\Delta\Psi m$ as they are selectively sequestered by respiring mitochondria by virtue of their negative charges on the inner membrane and are washed out when $\Delta\Psi m$ is lost. As shown in Fig. 4A, the extent of CMXRos staining in pEGFP53BP2-transfected cells (visualized by the expression of GFP)

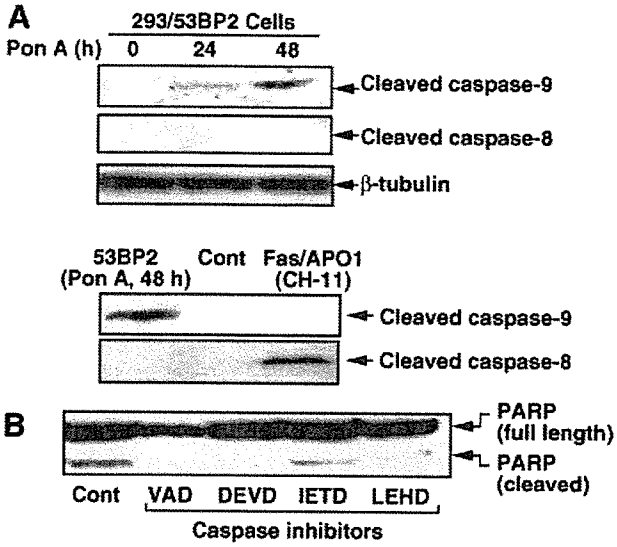

Figure 5 Involvement of caspase-9 in apoptosis induced by 53BP2S. (A) Activation of caspase-9 by 53BP2S. 293/53BP2 cells were treated by pon A (5 μM) for the indicated periods (h). Each cell lysate (10 μg protein) was examined for the activated ('cleaved') form of caspase-9 by Western blotting with anti-caspase-9 (cleaved form) or anti-caspase-8 (cleaved form) antibodies (upper panel). β-tubulin was used as an internal control. In the lower panel, 293/53BP2 cells were either stimulated with the agonistic anti-Fas antibody (CH-11) or treated with pon A and the activation of caspase-8 or caspase-9 was similarly examined. (B) Inhibition of the PARP cleavage by caspase inhibitors. 293/53BP2 cells were cultured with or without caspase inhibitors for 12 h and treated with pon A (5 μM) for 48 h. The cell lysate was prepared and examined for the PARP cleavage by Western blotting. The same amounts of each cell lysate (10 μg protein) were analyzed. Cont, DMSO alone; VAD, common inhibitor for the caspase-family (Z-VAD-FMK); DEVD, caspase-3-specific inhibitor (Z-DEVD-FMK); IETD, caspase-8-specific inhibitor (Z-IETD-FMK); LEHD, caspase-9-specific inhibitor (Z-IETD-FMK).

was diminished, indicating a decrease in $\Delta\Psi m$. In contrast, no such changes were observed in the control cells transfected with pEGFP. In Fig. 4B, the temporal change of $\Delta\Psi m$ in 293/53BP2 cells is shown. When 53BP2S was expressed, progressive reduction of $\Delta\Psi m$ detected by the rhodamine123 fluorescence intensity was observed over time, concomitantly with the appearance of apoptotic cells (compare with Fig. 2B). No such change was observed in control 293/LZ cells.

Involvement of caspase-9 in apoptosis induced by 53BP2S

Finally, to examine the upstream caspase cascade involved in the 53BP2S-mediated apoptosis, 293/53BP2 cell lysates were prepared after 24 and 48 h of pon A treatment. The presence of activated (cleaved) forms of caspase-8 and caspase-9 were examined in these cells. Figure 5A shows that caspase-9, but not caspase-8, was activated following the induction of 53BP2S. To confirm these observations, the effects of specific inhibitors for caspase-3, -8, and -9 were examined. As shown in Fig. 5B, the effects of peptide inhibitors among all types of known caspases (VAD), caspase-3 (DEVD), caspase-8 (IETD) and caspase-9 (LEHD) were shown. Although VAD, DEVD and LEHD effectively blocked the PARP cleavage induced by 53BP2S, only a minimal effect was observed with IETD. These findings indicate that 53BP2S induces apoptosis through the mitochondrial ('intrinsic') death pathway.

Discussion

The present data have revealed the involvement of mitochondria in the 53BP2-mediated apoptosis. 53BP2 has two protein isoforms, 53BP2S and 53BP2L, generated by alternative splicing (Takahashi *et al.* 2004). These two 53BP2 proteins are localized predominantly in the cytoplasm and exhibited similar biological actions although we do not currently know the reason of such redundancy. In this study, we have explored the proapoptotic action of 53BP2S using transient expression and the stable cell line in which 53BP2 is under the stringent control of pon A. When expressed, 53BP2S was located in the mitochondria and induced cell death associated with $\Delta\Psi m$ repression, caspase-9 activation, PARP cleavage, annexin V staining, and typical nuclear morphology, suggesting the involvement of intrinsic death pathway.

Regarding the possible involvement of 53BP2 in the cellular response to DNA damage, we have previously reported the positive correlation between the level of 53BP2 mRNA expression and the sensitivity to DNA damaging agents in various human cancer cell lines although no mutation of 53BP2 gene was detected (Mori *et al.* 2000). In addition, Ao *et al.* (2001) found that 53BP2S expression augmented the cellular apoptotic response to the DNA damage. Lopez *et al.* (2000) observed that the DNA damage induced the 53BP2 expression and protein stabilization leading to apoptosis. Bergamaschi *et al.* (2004) recently reported similar observations with ASPP2 (53BP2L). Therefore, it is likely that the activated p53 may augment the 53BP2-mediated cell death. In support of this action of p53, Marchenko *et al.* (2000) demonstrated the mitochondrial translocation of p53 upon irradiation and induction of apoptosis through the intrinsic death pathway. Mihara *et al.* (2003) further explored the mitochondrial involvement of p53 and found that p53 formed a complex with

Bcl-2 and $BclX_L$ followed by permeabilization of the outer mitochondrial membrane.

Intriguingly, Iwabuchi *et al.* (1998) and Samuels-Lev *et al.* (2001) found that p53-mediated transactivation was augmented by 53BP2S and 53BP2L (ASPP2), respectively. Samuels-Lev *et al.* (2001) proposed a model that 53BP2L interacts with p53 in the nucleus and specifically enhances gene expression of p53 responsive pro-apoptotic genes such as Bax. Although the 3D structure model of p53 and 53BP2 complex (Gorina & Pavletich 1996) does not support their hypothesis because when 53BP2 binds to p53, it involves the L3 loop of p53 (required for its DNA binding) and the H1 helix (required for p53 dimerization), thus precluding the p53 binding to DNA, there may be multiple mechanisms by which 53BP2 induces apoptosis.

In addition to the possible involvement of p53 and 53BP2 in apoptosis, 53BP2 abnormality is implicated in autoimmunity such as systemic lupus erythematosus (SLE) since one of the genetic loci of the familial incidence of SLE was shown to be located to 1q42.1 (Tsao *et al.* 1997), to which *TP53BP2* is located (Yang *et al.* 1997). This is coincided with the fact that abnormalities of various apoptosis-associated factors were reported in SLE and its animal models (Fisher *et al.* 1995; Sneller *et al.* 1997; Jackson & Puck 1999). Further genetic studies are needed to find a link between 53BP2 and autoimmunity.

Our observations together with those of others suggest that 53BP2 is involved in apoptosis at multiple steps and is implicated in various pathological processes. Since 53BP2 has been shown to interact with a number of proteins responsible for the regulation of apoptosis such as p53, Bcl-2 and NF-κB p65 subunit, selective interaction of 53BP2 with these proteins may determine the susceptibility of cells to trigger the apoptotic pathway.

Experimental procedures

Reagents and antibodies

FuGENE 6 and SuperFect transfection reagents were purchased from Roche Molecular Biochemicals (Indianapolis, IN, USA) and QIAGEN (Qiagen Inc., Valencia, CA, USA), respectively. PE-conjugated annexin V and 7-AAD (Becton Dickenson, Mountain View, CA, USA), ponasterone A (pon A) (Invitrogen, La Jolla, CA, USA) were commercially obtained. The caspase inhibitors (caspase-3 inhibitor, Z-DEVD-FMK; caspase-8 inhibitor, Z-IETD-FMK; caspase-9 inhibitor, Z-LEHD-FMK; caspase-family inhibitor, Z-VAD-FMK) were purchased from MBL. Mouse monoclonal antibodies to human 53BP2 (BD Transduction Laboratories, San Diego, CA, USA), β-tubulin (Sigma Chemical Co., St. Louis, MO, USA), human lactate dehydrogenase (LDH) (MBL, Nagoya, Japan) and human Fas (Sigma), and mouse polyclonal antibody to human mitochondrial heat shock protein 70 (Affinity Bioreagents, Golden, CO, USA) were purchased from individual suppliers. The rabbit polyclonal antibody to human 53BP2 was a generous gift from L. Naumovski (Stanford University, CA, USA). Mouse monoclonal antibodies to caspase-8 (cleaved form) and caspase-9 (cleaved form) and rabbit polyclonal antibody to PARP were purchased from Cell Signaling Technology (Beverly, MA, USA).

Plasmids

Construction of the 53BP2S expression plasmids, pcDNA3.1–53BP2 and pEGFP-53BP2, expressing 53BP2S protein (1005 amino acids) either alone or in fusion with green fluorescence protein (GFP), was reported previously (Yang *et al.* 1999). pCEP4-ASPP2, expressing 53BP2L (1128 amino acids), was a gift from L. Naumovski. pDsRed2-Mito, expressing a fusion protein of the *Discosoma* sp. red fluorescent protein linked to the mitochondrial targeting sequence from subunit VIII of human cytochrome oxidase, was purchased from BD Bioscience Clontech (Palo Alto, CA, USA).

Cell lines and cultures

The 53BP2S inducible cell line 293/53BP2 and its control cell line 293/LZ were kindly provided by Charles D. Lopez, Stanford University, CA, USA and previously described (Lopez *et al.* 2000). These cells were grown at 37 °C in 5% CO_2 in Dulbecco's modified Eagle medium (DMEM) with 10% (v/v) heat-inactivated foetal calf serum, 290 μg/mL of L-glutamine, 100 U/mL penicillin, 100 μg/mL streptomycin, 600 μg/mL G418 and 500 μg/mL Zeocin. The parental 293 and HeLa cells were grown at 37 °C in DMEM with 10% (v/v) heat-inactivated foetal calf serum (IBL, Maebashi, Japan), 1 mM glutamate, 100 U/mL penicillin, and 100 μg/mL streptomycin. A human pancreatic cancer cell line MIA PaCa-2 was grown in Eagle minimal essential medium supplemented with nonessential amino acids, 10% (v/v) heat-inactivated foetal calf serum, 100 U/mL penicillin, and 100 μg/mL streptomycin.

Immunostaining

Semi-confluent MIA PaCa-2 cells on Laboratory-Tek tissue culture chamber slides were fixed with 4.5%

paraformaldehyde in PBS for 15 min at room temperature, rinsed twice with PBS, and incubated with PBS containing 0.5% Triton X-100 for 20 min at room temperature. They were subsequently incubated with the primary anti-53BP2 mouse antibody (B92320, Transduction Laboratories, Lexington, KY, USA) for 1 h at 37 °C, rinsed three times with PBS containing 0.05% Triton X-100, and incubated with the secondary antibody, rhodamine-conjugated goat anti-mouse IgG (Calbiochem-Novabiochem, La Jolla, CA, USA), for 1 h at 37 °C. The slides were rinsed with PBS three times and mounted with buffered glycerol for fluorescent microscopic examination. Primary and secondary antibodies were diluted at 1 : 100 and 1 : 200, respectively, in PBS containing 3% bovine serum albumin.

Cell fractionation

In order to examine the cellular localization of 53BP2 in the 293/53BP2 cells, cells were pretreated with pon A (5 μM, 48 h) and subjected to fractionation using commercial kits (Nuclear/Cytosol Fractionation Kit and Mitochondria/Cytosol Fractionation Kit, BioVision, Mountain View, CA, USA). The heavy membrane precipitate containing mitochondria was extensively washed in order to avoid the contamination of cytoplasmic proteins. The identification of 53BP2 and validation of cell fractionation were performed by Western blotting with antibodies to 53BP2, LDH (cytoplasmic marker) and mitochondrial heat shock protein 70 (mitochondria marker).

Flow cytometric analysis of apoptosis

In order to assess apoptosis, flow cytometric analysis was performed using FACScan (Becton Dickinson). MIA PaCa-2 cells were transiently transfected with pcDNA3.1–53BP2 expressing 53BP2S or pCEP4-ASPP2 expressing 53BP2L using SuperFect according to the manufacturer's recommendations. Cells at a concentration of approximately 1×10^6 cells/mL were washed twice with cold PBS and resuspended in annexin V binding buffer (10 mM HEPES-NaOH (pH 7.4), 140 mM NaCl and 2.5 mM $CaCl_2$). In some experiments, cells were double-stained with annexinV and 7-Amino-actinomycin D (7-AAD). 293/53BP2 cells were induced to express 53BP2 by incubation with 5 μM pon A and apoptotic cells were similarly counted.

Microscopic examination

In order to examine the cellular localization of 53BP2S, 293 cells were cultured on 2-well Laboratory-Tek tissue culture chamber slides and transfected with 0.4 μg of pEGFP-53BP2 expressing 53BP2S together with 0.1 μg of the mitochondria targeting plasmid, pDsRed2-Mito (BD Bioscience Clontech). The transfected cells were fixed with 4.0% paraformaldehyde in PBS for 15 min at room temperature, and observed under the confocal microscope (RADIANCE2000; Bio-Rad, Hercules, CA, USA). Each fluorophore was recorded separately using narrow-band filters centered at 522 nm for GFP fluorescence and 605 nm for DsRed2 fluorescence.

Evaluation of apoptosis by Western blotting

Apoptosis was also assessed by the cleavage of PARP, and caspases-8 and -9 by Western blotting using relevant antibodies described above. Briefly, whole cell extracts were lyzed in 200 μL of ice-cold lysis buffer (50 mM Tris-HCl (pH 8.0), 100 mM NaCl, 5 mM EDTA, 50 mM sodium fluoride, 2 mM dithiothreitol, 0.25% Nonidet P-40, 1 mM phenylmethyl-sulfonyl fluoride, 10 μg/mL aprotinin, 10 μg/mL leupeptin and 1 μg/mL pepstatin (A). The lysate was cleared by centrifugation and the protein concentration of the whole cell extract was measured using Bio-Rad DC protein assay kit (Bio-Rad). Equal amounts of cell lysates (10 μg protein) were resolved by 10% SDS-PAGE and transferred on nitrocellulose membrane followed by incubating with individual antibodies. The immunoreactive proteins were visualized by ECL.

Determination of mitochondrial $\Delta\Psi$m in cultured cells

To evaluate $\Delta\Psi$m, cells were treated with 10 μg/mL Rh123 for 15 min at 37 °C. After incubation, cells were washed with PBS(+) three times, resuspended in PBS(+), and fluorescence was scored immediately by flow cytometer. To visualize the cells with depressed $\Delta\Psi$m, cells growing on Laboratory-*Tek*II chambered cover glass were stained with 40 nM CMXRos in PBS(+) for 15 min, washed with PBS(+) three times and observed under the confocal microscope (Bio-Rad MRC600UVF). The acquisitions of the mitochondrial images were provided by 585LP emission filter with same setting (Iris: 2.0, Gain: 1.4).

Acknowledgments

We thank Dr Louie Naumovski (Stanford University) for his generous gifts of 293/53BP2 cells, polyclonal antibody to 53BP2, and a plasmid expressing 53BP2L. This work was supported in part by grants-in-aid from the Ministry of Health, Labor and Welfare, the

Ministry of Education, Culture, Sports, Science and Technology of Japan and Japanese Human Sciences Foundation.

References

Ao, Y., Rohde, L.H. & Naumovski, L. (2001) p53-interacting protein 53BP2 inhibits clonogenic survival and sensitizes cells to doxorubicin but not paclitaxel-induced apoptosis. *Oncogene* **20**, 2720–2725.

Bergamaschi, D., Samuels, Y., Jin, B., Duraisingham, S., Crook, T. & Lu, X. (2004) ASPP1 and ASPP2: Common activators of p53 family members. *Mol. Cell. Biol.* **24**, 1341–1350.

Daniel, N.N. & Korsmeyer, S.J. (2004) Cell death: Critical control points. *Cell* **116**, 205–219.

Fisher, G.H., Rosenberg, F.J., Straus, S.E., *et al.* (1995) Dominant interfering Fas gene mutations impair apoptosis in a human autoimmune lymphoproliferative syndrome. *Cell* **81**, 935–946.

Gorina, S. & Pavletich, N.P. (1996) Structure of the p53 tumor suppressor bound to the ankyrin and SH3 domains of 53BP2. *Science* **274**, 1001–1005.

Green, D.R. & Reed, J.C. (1998) Mitochondria and apoptosis. *Science* **281**, 1309–1312.

Iwabuchi, K., Bartel, P.L., Li, B., Marraccino, R. & Fields, S. (1994) Two cellular proteins that bind to wild-type but not mutant p53. *Proc. Natl. Acad. Sci. USA* **91**, 6098–6102.

Iwabuchi, K., Li, B., Massa, H.F., Trask, B.J., Date, T. & Fields, S. (1998) Stimulation of p53-meditated transcriptional activation by the p53-binding proteins, 53BP1 and 53BP2. *J. Biol. Chem.* **273**, 26061–26068.

Jackson, C.E. & Puck, J.M. (1999) Autoimmune lymphoproliferative sundrome, a disorder of apoptosis. *Curr. Opin. Pediatr.* **11**, 521–527.

Judith, H.M., Caroline, D., Jean, C.M. & James, D. (2004) Role of mitochondrial membrane permeabilization in apoptosis and cancer. *Oncogene* **23**, 2850–2860.

Lopez, C.D., Ao, Y., Rohde, L.H., *et al.* (2000) Proapoptotic p53-interacting protein 53BP2 is induced by UV irradiation but suppressed by p53. *Mol. Cell. Biol.* **20**, 8018–8025.

Marchenko, N.D., Zaika, A. & Moll, U.M. (2000) Death signal-induced localization of p53 protein to mitochondria. A potential role in apoptotic signaling. *J. Biol. Chem.* **275**, 16202–16212.

Mihara, M., Erster, S., Zaika, A., *et al.* (2003) p53 has a direct apoptogenic role at the mitochondria. *Mol. Cell* **11**, 577–590.

Mori, T., Okamoto, H., Takahashi, N., Ueda, R. & Okamoto, T. (2000) Aberrant overexpression of 53BP2 mRNA in lung cancer cell lines. *FEBS Lett.* **465**, 124–128.

Naumovski, L. & Cleary, M.L. (1996) The p53-binding protein 53BP2 also interacts with Bc12 and impedes cell cycle progression at G2/M. *Mol. Cell. Biol.* **16**, 3884–3892.

Samuels-Lev, Y., O'Connor, D.J., Bergamaschi, D., *et al.* (2001) ASPP proteins specifically stimulate the apoptotic function of p53. *Mol. Cell* **8**, 781–794.

Sneller, M.C., Wang, J., Dale, J.K., *et al.* (1997) Clinical, immunologic, and genetic features of an autoimmune lymphoproliferative syndrome associated with abnormal lymphocyte apoptosis. *Blood* **89**, 1341–1348.

Takahashi, N., Kobayashi, S., Jiang, X., *et al.* (2004) Expression of 53BP2 and ASPP2 proteins from TP53BP2 gene by alternative splicing. *Biochem. Biophys. Res. Commun.* **315**, 434–438.

Tsao, B.P., Canto, R.M., Kalunian, K.C., *et al.* (1997) Evidence for linkage of a candidate chromosome 1 region to human systemic lupus erythematosus. *J. Clin. Invest.* **99**, 725–731.

Yang, J.P., Ono, T., Sonta, S., Kawabe, T. & Okamoto, T. (1997) Assignment of p53 binding protein (TP53BP2) to human chromosome band 1q42.1 by in situ hybridization. *Cytogenet. Cell Genet.* **78**, 61–62.

Yang, J.P., Hori, M., Takahashi, N., Kawabe, T., Kato, H. & Okamoto, T. (1999) NF-κB subunit p65 binds to 53BP2 and inhibits cell death induced by 53BP2. *Oncogene* **18**, 5177–5186.

Received: 8 October 2004
Accepted: 12 December 2004

Inhibition of the 53BP2S-mediated apoptosis by nuclear factor κB and Bcl-2 family proteins

Naoko Takahashi[1], Shinya Kobayashi[1], Shinichi Kajino[1], Kenichi Imai[1], Keisuke Tomoda[1], Shigeomi Shimizu[2] and Takashi Okamoto[1,*]

[1]*Department of Molecular and Cellular Biology, Nagoya City University Graduate School of Medical Sciences, 1 Kawasumi, Mizuho-cho, Mizuho-ku, Nagoya, Aichi 467-8601, Japan*

[2]*Laboratory of Molecular Genetics, Osaka University Medical School, 2-2 Yamadaoka, Suita, Osaka 565-0871, Japan*

The p53 binding protein 2 (53BP2) has been identified independently as the interacting protein to p53, Bcl-2, and p65 subunit of nuclear factor κB (NF-κB). It was demonstrated that over-expression of 53BP2 (renamed as 53BP2S) induces apoptotic cell death. In this study we explored the effect of NF-κB activation elicited by a physiological NF-κB inducer, interleukin-1β (IL-1β), and anti-apoptotic Bcl-2 family proteins on the 53BP2S-mediated apoptosis. We found that both NF-κB activation and Bcl-2 family proteins could prevent the 53BP2S-mediated depression of mitochondrial transmembrane potential, activation of caspase-9, cleavage of poly ADP ribose polymerase (PARP), and cell death. These observations suggested that 53BP2S/Bbp and its directly or indirectly interacting proteins might play crucial roles in the regulation of apoptosis and contribute to carcinogenesis. It is also suggested that 53BP2S/Bbp induces apoptosis through the mitochondrial death pathway presumably by counteracting the actions of anti-apoptotic Bcl-2 family proteins. The regulatory network of the 53BP2S-mediated apoptosis cascade including its interacting proteins is discussed.

Introduction

Although the p53 binding protein 2 (53BP2) was identified as one of the interacting proteins to p53 (Iwabuchi *et al.* 1994), subsequent studies found that it also interacts with Bcl-2 (Naumovski & Cleary 1996) and p65 subunit of nuclear factor κB (NF-κB) (Yang *et al.* 1999), suggesting its role in carcinogenesis. We recently found that although the 53BP2 protein is encoded by a single copy gene *TP53BP2* located in the long arm of chromosome 1 at q42.1 (Yang *et al.* 1997), two isoform proteins, 53BP2S and 53BP2L, formerly named 53BP2 (Yang *et al.* 1999) or Bcl-2 binding protein (Bbp) (Naumovski & Cleary 1996) and ASPP2 (Samuels-Lev *et al.* 2001), respectively, are generated by alternative splicing (Takahashi *et al.* 2004). We and others reported the proapoptotic action of 53BP2S/Bbp by demonstrating the annexin V staining, nuclear fragmentation, and induction of cell death (Yang *et al.* 1999; Lopez *et al.* 2000; Ao *et al.* 2001; Samuels-Lev *et al.* 2001; Bergamaschi *et al.* 2004). In addition, we have recently found that 53BP2S/Bbp is translocated to the mitochondria and induces cell death through the mitochondrial death pathway (Kobayashi *et al.* 2005).

53BP2 proteins interact with p53, p65 and Bcl-2 through the C-terminal ankyrin repeats and SH3 domain (Iwabuchi *et al.* 1994; Naumovski & Cleary 1996; Yang *et al.* 1999). Previous studies indicated that the 53BP2 binding site in the p53 core domain is evolutionarily conserved and is frequently mutated in human cancer (Iwabuchi *et al.* 1994; Gorina & Pavletich 1996), suggesting that 53BP2 proteins may participate in the biological actions of p53. In fact, we found that the levels of 53BP2 mRNA expression in various human cancer cell lines was correlated with the sensitivity to DNA damaging agents irrespectively of the p53 status (Mori *et al.* 2000), indicating the biological relevance *in vivo*.

In this study, we have further explored the effects of NF-κB and Bcl-2 family proteins on the proapoptotic action of 53BP2S/Bbp. We found that both NF-κB and Bcl-2 family proteins could prevent the 53BP2S-mediated apoptosis. The biological roles of 53BP2 proteins and these interacting proteins in the regulation of apoptosis, and their possible roles in carcinogenesis are discussed.

Communicated by: Hideyuki Okano

**Correspondence*: E-mail: tokamoto@med.nagoya-cu.ac.jp

DOI: 10.1111/j.1365-2443.2005.00878.x

Results

Induction of apoptosis by 53BP2S

To assess the proapoptotic effect of 53BP2S/Bbp, we transfected 53BP2S gene in MIA PaCa-2 cells and the induction of apoptosis was evaluated by typical nuclear morphology and trypan blue dye exclusion assay. In Fig. 1A, when MIA PaCa-2 cells were transfected with pEGFP-53BP2 (Yang *et al.* 1999), expressing 53BP2S/Bbp, the typical apoptotic morphology, such as nuclear condensation and fragmentation, was observed in these transiently transfected cells. Approximately 32% of cells exhibited apoptosis when 53BP2S was transduced, which was significantly higher than the control (6.2%; $P < 0.01$) (Fig. 1B). To further confirm the effect of 53BP2S/Bbp, 293/53BP2 cells, a stable cell line in which 53BP2S/Bbp expression is under the stringent control of ponasteron A (pon A), were treated with pon A to induce 53BP2S/Bbp expression. After 24 h of postinduction, similar apoptotic nuclear changes were observed in 293/53BP2 cells whereas the control 293/LZ cells did not show such changes (Fig. 1C). In Fig. 1D, the number of surviving cells in 293/53BP2 and 293/LZ cultures were counted by trypan blue dye exclusion assay,

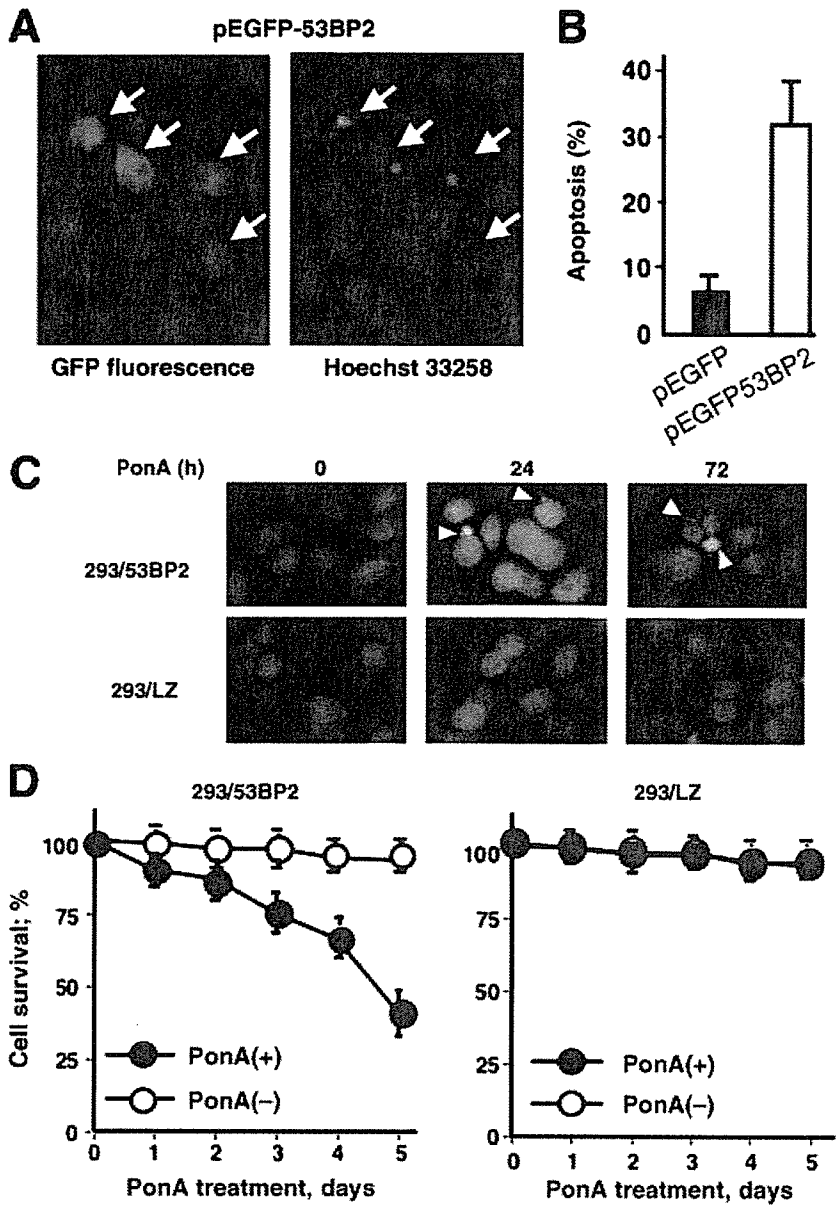

Figure 1 Induction of apoptosis by 53BP2S protein. (A) Nuclear morphology of 53BP2S-transfected cells. MIA PaCa-2 cells were transfected with pEGFP-53BP2, stained with Hoechst 33258, and observed under a fluorescence microscope. Arrows indicate the locations of transfected cells with typical nuclear morphology of apoptotic cells. (B) Quantification of the proapoptotic effect of 53BP2S. The percentage of apoptotic cells among the GFP stained cells is shown. ■ transfection with pEGFP (control); □ transfection with pEGFP-53BP2. (C) Nuclear morphology of apoptotic cells in 293/53BP2 upon 53BP2S/Bbp induction. The pon A-induced cells were stained with Hoechst-33258 and observed under a fluorescent microscopy. The apoptotic cells were identified by their fragmented and/or condensed nuclear morphology (indicated by arrowheads). (D) Induction of cell death by 53BP2S/Bbp. 293/53BP2 and 293/LZ (control) cells were stimulated with pon A (5 μM) for the indicated periods (in days) and stained with trypan blue. The surviving cells, not stained with trypan blue, were counted.

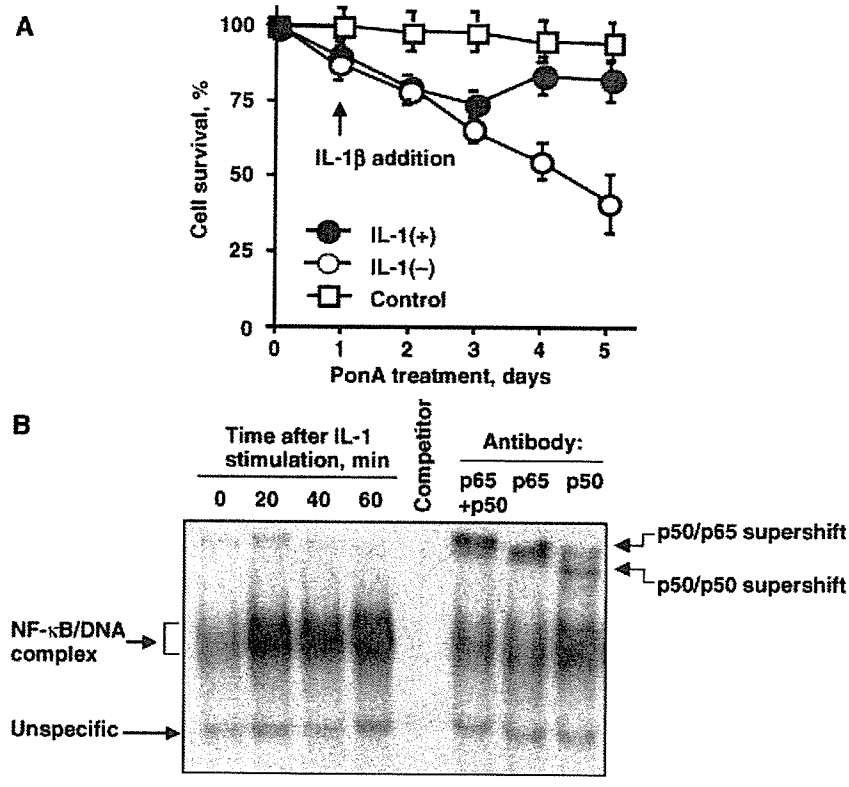

Figure 2 Inhibition of the 53BP2S-induced cell death by the treatment with IL-1β. (A) 293/53BP2 cells were treated with pon A (5 μM) and NF-κB was activated by IL-1β (20 ng/mL) after 1 day of pon A treatment. Cell survival rate was assessed by dye exclusion assay using trypan blue. After pon A treatment, cells were either stimulated with (●) or without IL-1β (○). Control (□), 293/53BP2 cells without pon A treatment. (B) Activation of NF-κB DNA-binding activity. 293/53BP2 cells were simulated with IL-1β (20 ng/mL) for indicated time periods and were harvested to prepare the nuclear extract for EMSA with the κB DNA probe. Supershift assays were performed by incubating the nuclear extract (40 min after IL-1β stimulation) with polyclonal antibodies against p65 and p50.

with or without pon A, over time following the induction. The survival rate of 293/53BP2 cells decreased upon 53BP2S/Bbp expression and reached 54%, whereas that of the untreated cells (without pon A) was only 3%, and was similar to the background level of control cells (293/LZ).

Inhibition of the 53BP2S-induced cell death by NF-κB activation

To examine the effect of NF-κB activation on the 53BP2S-induced cell death, IL-1β was added after the production of 53BP2S protein by ponA treatment for 24 h in 293/53BP2 cells. As shown in Fig. 2A, the 53BP2S-mediated cell death was prevented. There was a time lag of approximately 48 h between the addition of IL-1β and the appearance of inhibition of cell death. In the experiment demonstrated in Fig. 2A, 53(B)P2S protein was detectable after 12 h ponA treatment (data not shown). The NF-κB activation by IL-1β was monitored by the induction of its DNA binding activity as demonstrated by the electrophoretic mobility shift assay (EMSA) (Fig. 2B). Whereas the cell survival rate of the 53BP2S-expressing cells was 42% after 5 days of pon A treatment, that of the cells treated with IL-1β (24 h after the pon A treatment) exhibited an 84% survival rate, which was very close to the level of control 293/LZ cells not expressing 53BP2S/Bbp (Fig. 2A). The IL-1β treatment had no effect on the level of 53BP2S/Bbp expression *per se* in 293/53BP2 cells (data not shown). In addition, we detected expression of Bcl-2 and Bcl-X_L proteins and their levels were not further up-regulated by the IL-1β treatment (data not shown).

As shown in Fig. 3, the 53BP2S-induced cell death was associated with the cleavage of poly ADP ribose polymerase (PARP), a typical biochemical marker of apoptosis. It is also shown that the cleaved form of caspase-9 at 24 h after ponA treatment, but not caspase-8, was emerged, suggesting that the 53BP2S/Bbp induces cell death through the mitochondrial death pathway. No such changes were detected in the control 293/LZ cells (data not shown). However, when 293/53BP2 cells were treated with IL-1β, the PARP cleavage and the emergence of caspase-9 were prevented.

Inhibition of the 53BP2S-mediated apoptosis by Bcl-2 and Bcl-X_L

We then examined the effect of Bcl-2 family proteins on the 53BP2S-mediated apoptosis. Bcl-2, Bcl-X_L, and ΔBH4 mutant of Bcl-X_L lacking the crucial BH4 domain, were

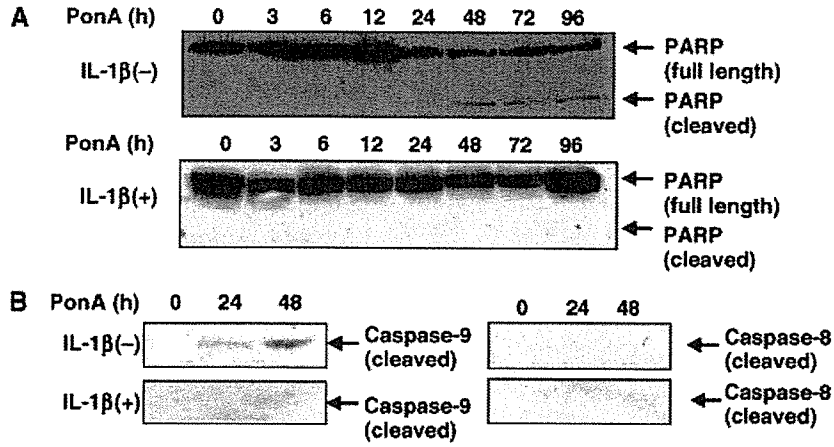

Figure 3 Inhibition of the 53BP2S-induced PARP cleavage by IL-1β treatment. (A) 293/53BP2 cells were pretreated with or without IL-1β (20 ng/mL) for 12 h and 53BP2S/Bbp expression was induced by pon A (5 μM). These cells were harvested for the examination of PARP cleavage by Western blotting with anti-PARP rabbit polyclonal antibody. The positions of the intact full-length PARP (116 kDa) and its cleaved form (89 kDa) are indicated by the arrows. Experiments were repeated three times and the same results were obtained. (B) Inhibition of caspase-9 activation by IL-1β. Pretreatment of 293/53BP2 cells with IL-1β and induction of 53BP2S/Bbp were similarly performed as above. The position of the activated ('cleaved') form of caspase-9 is indicated by the arrow. No activation of caspase-8 was detected by 53BP2 induction.

expressed together with 53BP2S/Bbp in MIA PaCa-2 cells and the number of apoptotic cells were counted. As shown in Fig. 4, both Bcl-2 and Bcl-X_L expression inhibited 53BP2S-induced cell death in a dose-dependent manner, with greater inhibitory effect of Bcl-X_L. No such effect was observed with ΔBH4 mutant.

Since these anti-apoptotic Bcl-2 proteins are known to block cell death by restoring the mitochondrial membrane potential ($\Delta\Psi m$), we examined $\Delta\Psi m$ of the transfected cells by staining with a fluorescence dye CMX-ROS (Fig. 5). Whereas 53BP2S/Bbp induced the reduction of $\Delta\Psi m$, observed by the reduction of mitochondrial staining with CMX-ROS, expression of Bcl-2 or Bcl-X_L, but not ΔBH4 mutant, prevented its reduction. These results confirmed the anti-apoptotic effect of anti-apoptotic Bcl-2 proteins shown in Fig. 4.

Discussion

The present data have revealed the inhibitory effects of NF-κB and Bcl-2 family proteins on the 53BP2S-mediated apoptosis. The partial clone of 53BP2 was initially identified as one of the interacting proteins of p53 (Iwabuchi *et al.* 1994). Since NF-κB p65 subunit and Bcl-2 are known to inhibit apoptosis (DeLuca *et al.* 1998; Haddad 2004) and have previously been reported to interact with 53BP2S/Bbp (Naumovski & Cleary 1996; Yang *et al.* 1999), our findings indicate that anti-apoptotic actions of these proteins appear to be through blocking the pro-apoptotic actions of 53BP2S/Bbp at least in a part. Thus, 53BP2S-mediated apoptosis is regulated by p53, NF-κB and Bcl-2/Bcl-X_L (Fig. 6).

Because of its localization and negative regulation by anti-apoptotic Bcl-2 family proteins, it is suggested that 53BP2S/Bbp induces apoptosis by stimulating the effect of intrinsic (mitochondrial) death pathway mediated by proapoptotic Bcl-2 family proteins or by blocking the actions of anti-apoptotic Bcl-2 family proteins. Since 53BP2S/Bbp is known to interact with Bcl-2 at least *in vitro* as well as in yeast cells (Naumovski & Cleary 1996), and Bcl-X_L and Bcl-2 exhibit a high structural and functional similarity, it is possible that 53BP2S/Bbp can interfere with actions of these anti-apoptotic Bcl-2 family proteins. However, we and others failed to detect the protein–protein interaction of 53BP2S/Bbp and these Bcl-2 proteins in cells (data not shown). Thus, further studies are needed to address this possibility. From experimental observations so far obtained, we speculate that 53BP2 may down-modulate the cell death 'rheostat' (Daniel & Korsmeyer 2004), that is maintained by the balance between pro-apoptotic and anti-apoptotic Bcl-2 proteins (Haddad 2004) and set the threshold of susceptibility to apoptosis, by blocking the action of anti-apoptotic Bcl-2 family proteins at the vicinity of mitochondria (Fig. 6).

It is not clear whether p53 is required for the proapoptotic action of 53BP2 proteins. Lopez *et al.* (2000) observed that the DNA damage induced the 53BP2S/

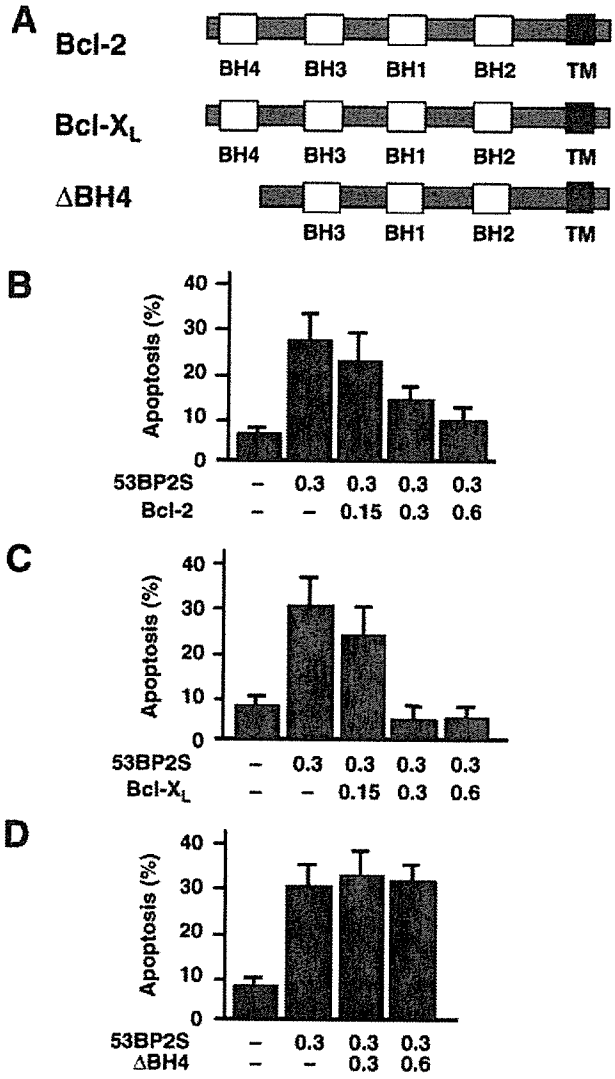

Figure 4 Attenuation of 53BP2S-induced apoptosis by Bcl-2 and Bcl-X_L. (A) The schematic representation of Bcl-2 proteins used in this study. (B, C, D) Effects of Bcl-2 proteins on the 53BP2S-mediated apoptosis. MIA PaCa-2 cells were transfected with pcDNA3.1-53BP2, expressing 53BP2S/Bbp, together with pCAGGA-Bcl-2, pCAGGA-Bcl-X_L or pCAGGA–ΔBH4, and apoptotic cells were counted. The average and the S.D. values of four independent experiments are shown. Note that no effect was observed with the Bcl-X_L mutant (ΔBH4). The amounts (μg) of each plasmid are indicated.

Bbp expression and protein stabilization leading to apoptosis in the context of wild-type p53, although p53 suppressed 53BP2S/Bbp expression in undamaged cells. We and others have previously reported very low 53BP2 protein levels in spite of the highly abundant mRNA and suggested a possibility that the 53BP2 level might be regulated at the post-translational level (Naumovski & Cleary 1996; Yang *et al.* 1999; Lopez *et al.* 2000). Thus, the p53 interaction may stabilize 53BP2 proteins and enhance its apoptotic action. In addition, it was reported that p53-mediated transactivation was augmented by 53BP2S/Bbp (Iwabuchi *et al.* 1998) and 53BP2L/ASPP2 (Samuels-Lev *et al.* 2001). Samuels-Lev *et al.* (2001) proposed a model in which 53BP2L/ASPP2 interacts with p53 in the nucleus and specifically enhances gene expression of p53 responsive proapoptotic genes such as Bax. However, although MIA PaCa-2 cells contain p53 mutation at R248 (Yoshikawa *et al.* 1999), known to be involved in the interaction with 53BP2 at least in a crystal structure of the p53–53BP2 protein complex (Gorina & Pavletich 1996), we found that 53BP2S/Bbp could induce apoptosis in MIA PaCa-2 cells much more efficiently than in 293 cells, expressing wild-type p53 (Fig. 1). Thus, it is yet to be investigated whether 53BP2-mediated apoptosis requires the interaction with p53 and whether 53BP2S/Bbp and 53BP2L/ASPP2 have distinct actions in cells. It is also possible that proapoptotic actions of 53BP2 proteins are exerted at multiple levels.

We confirmed the inhibitory effect of NF-κB activation on the proapoptotic action of 53BP2S/Bbp. We demonstrate that anti-apoptotic action of NF-κB was evident even after the initiation of 53BP2S-mediated cell death (Fig. 2). The anti-apoptotic nature of NF-κB has been well established (DeLuca *et al.* 1998; Chen *et al.* 2001; Karin & Lin 2002). There are at least two mechanisms by which NF-κB inhibits apoptosis: (i) by induction of gene expression of anti-apoptotic proteins such as c-IAP2 (Chu *et al.* 1997), IEX-1 L (Wu *et al.* 1998) and even Bcl-X_L (Chen *et al.* 2000) and (ii) through blocking the action of proapoptotic factors by direct or indirect interaction (Yang *et al.* 1999). However, these two distinct mechanisms are not mutually exclusive for neither one mechanism alone can fully explain the strong anti-apoptotic action of NF-κB. In suppor of the latter mechanism, we observed that NF-κB could inhibit the TNF-α-mediated apoptosis without *de novo* protein synthesis at least in some cell lines (Kajino *et al.* 2000). Although the intracellular location where NF-κB interacts with 53BP2S/Bbp is not known, it may occur in the vicinity of mitochondria since NF-κB and IκBα are found in the mitochondrial intermembrane space and TNF-α can liberate the NF-κB within mitochondria (Bottero *et al.* 2001; Cogswell *et al.* 2003). Thus, 53BP2S/Bbp could serve as one of the molecular targets for the anti-apoptotic actions of NF-κB. However, since the delay of the anti-apoptotic effect of IL-1β on 53BP2S-mediated apoptosis was observed, it is possible that both

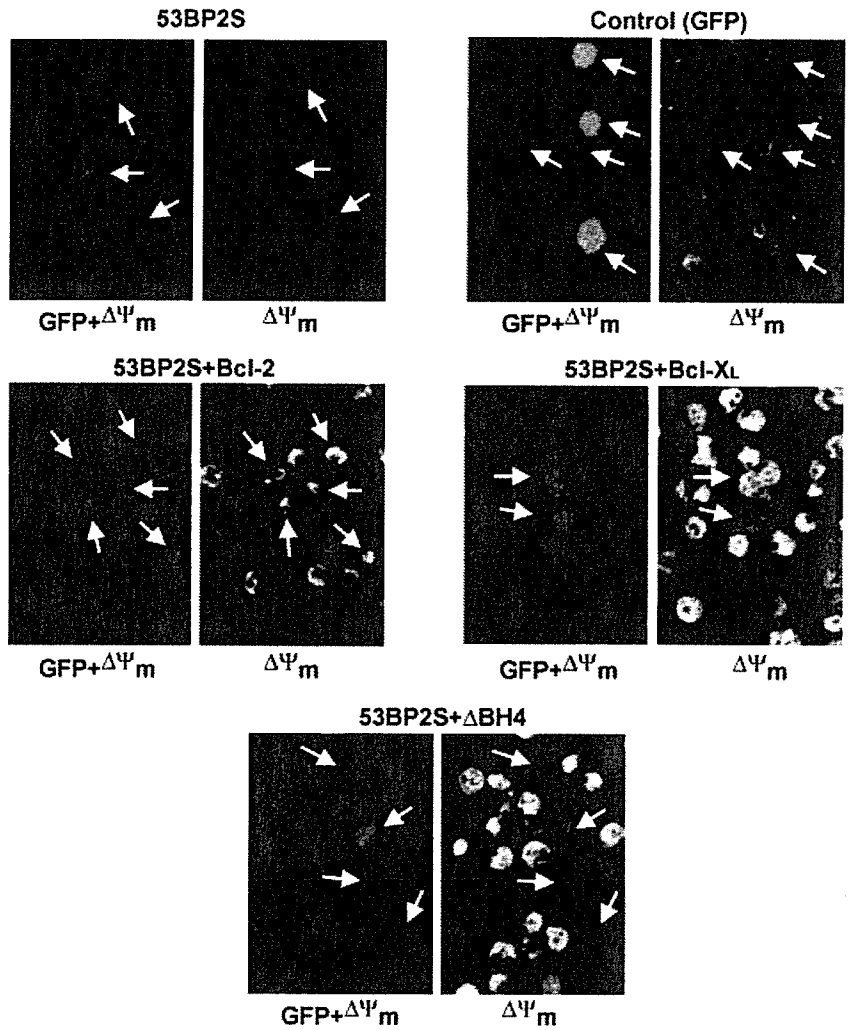

Figure 5 Restoration of ΔΨm depression on 53BP2S induction by Bcl-2 or Bcl-X_L. MIA PaCa-2 cells were transfected with pEGFP- 53BP2 or pEGFP (control). Effects of co-transfection with pUC-CAGGS-Bcl-2, pUC-CAGGS-Bcl-X_L or pUC-CAGGS-ΔBH4 were examined. Twenty-eight hours after the transfection, the cells were stained with CMX-ROS and the Δψm was observed under the confocal microscope. Figures on the left represent merged images of GFP (53BP2S/Bbp) staining (green) and CMX-ROS (Δψm) staining (red) and those on the right represent the CMX-ROS fluorescence on the right for clarity. Arrows indicate the locations of transfected (GFP-stained) cells. All figures were viewed in the same conditions (CMX-ROS concentration, fixation procedure, and exposure time for microscopic examination).

direct and indirect effects of NF-κB actions are involved in 53BP2S-induced apoptosis.

These observations have indicated the role of NF-κB in various pathologies and implicated NF-κB as a common therapeutic target (Karin & Lin 2002). For example, Arlt *et al.* (2002) reported that the blockade of NF-κB activation cascade by its inhibitors MG132 and sulfasalazine greatly augmented the effect of doxorubicin or etoposide in inducing the cell death of human pancreatic cancer cell lines. Use of these compounds and derivatives is expected to augment the therapeutic efficacy of conventional cancer therapy.

These findings support a possibility that 53BP2 proteins are involved in various biological processes such as carcinogenesis and the cellular response to DNA damage. Mori *et al.* (2000) reported that the level of 53BP2 mRNA expression in various human cancer cell lines was correlated with the sensitivity to DNA damaging agents although no mutation of 53BP2 gene was detected. In addition, Ao *et al.* (2001) observed that 53BP2S/Bbp expression augmented the cellular apoptotic response to the DNA damage. Thus, selective action of 53BP2 with p53, Bcl-2 and NF-κB p65 subunit may determine the susceptibility of cells to trigger the apoptotic pathway in response to the DNA damage (Fig. 6).

Experimental procedures

Reagents and antibodies

Human recombinant cytokine IL-1β (Boehringer Mannheim, Mannheim, Germany), Hoechst-33258 (Molecular Probes, Eugene, OR, USA), CMX-ROS (Molecular Probes), Ponasterone A (pon A) (Invitrogen, La Jolla, CA, USA) were commercially obtained. SuperFect transfection reagents was purchased from QIAGEN (Qiagen Inc., Valencia, CA, USA). Mouse monoclonal antibodies to human 53BP2 proteins (BD Transduction Laboratories,

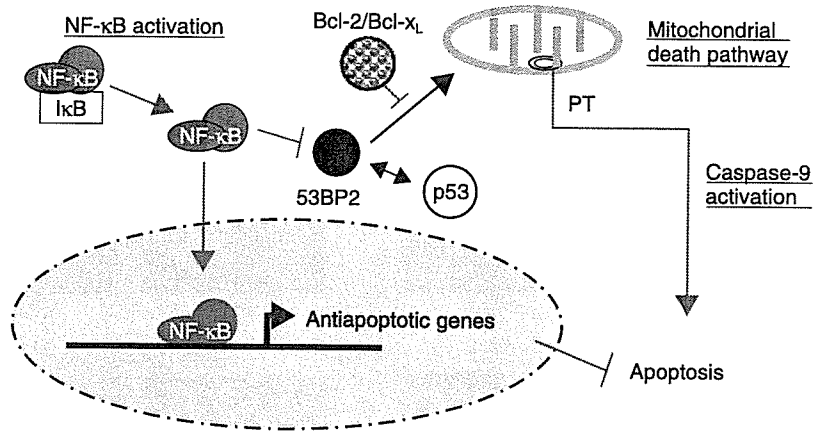

Figure 6 Regulation of the 53BP2S-mediated apoptosis by NF-κB and Bcl-2/Bcl-X_L. Previous findings indicate that p53 interacts with 53BP2 proteins to activate the proapoptotic action. Our findings indicate that NF-κB and Bcl-2/Bcl-X_L appear to block this action of 53BP2S/Bbp. The selective action of 53BP2S/Bbp with these proteins may determine the threshold of the cellular susceptibility to the intrinsic death pathway. See Discussion for the details.

San Diego, CA, USA), and rabbit polyclonal antibody to human p65 (Santa Cruz Biotech, Santa Cruz, CA, USA), goat polyclonal antibody to human p50 (Santa Cruz Biotech) were purchased from individual suppliers. The rabbit polyclonal antibody to human 53BP2 was a generous gift from L. Naumovski (Stanford University, CA, USA). Mouse monoclonal antibodies to caspase-8 (cleaved form) and caspase-9 (cleaved form) and rabbit polyclonal antibody to PARP were purchased from Cell Signaling Technology (Beverly, MA, USA).

Plasmids

Construction of the 53BP2S/Bbp expression plasmids, pcDNA3.1–53BP2 and pEGFP-53BP2, expressing 53BP2S/Bbp protein (1005 amino acids) either alone or in fusion with green fluorescence protein (GFP), was reported previously (Yang *et al.* 1999). Human bcl-2, bcl-x_L, and bclx_L mutant (ΔBH4) cDNAs were subcloned into the pUC-CAGGS expression vector as previously described (Shimizu *et al.* 1996, 2000).

Cell lines and cultures

The 53BP2S/Bbp inducible cell line 293/53BP2 and its control cell line 293/LZ were kindly provided by Charles D. Lopez, Stanford University, CA, USA and previously described (Lopez *et al.* 2000). These cells were grown at 37 °C in 5% CO_2 in Dulbecco's modified Eagle medium (DMEM) with 10% (v/v) heat-inactivated fetal calf serum, 290 μg/mL of L-glutamine, 100 U/mL penicillin, 100 μg/mL streptomycin, 600 μg/mL G418 and 500 μg/mL Zeocin. A human pancreatic cancer cell line MIA PaCa-2 was grown in Eagle minimal essential medium supplemented with nonessential amino acids, 10% (v/v) heat-inactivated fetal calf serum, 100 U/mL penicillin, and 100 μg/mL streptomycin.

Microscopic examination

In order to examine the apoptotic cell morphology, 293/53BP2 cells were cultured on 2-well Laboratory-Tek tissue culture chamber slides (Nunc, Inc., Naperville, IL, USA) and stimulated by pon A. The cells were fixed with 4.0% paraformaldehyde in PBS for 15 min at room temperature, rinsed twice in PBS and stained with Hoechst-33258. The apoptotic cells were identified by their shrunken morphology and the condensed and fragmented nuclear morphology.

Evaluation of apoptosis by Western blotting

Apoptosis was also assessed by the cleavage of PARP, and caspases-8 and -9 by Western blotting using relevant antibodies described above. Briefly, whole cell extracts were lyzed in 200 μL of ice-cold lysis buffer (50 mM Tris-HCl (pH 8.0), 100 mM NaCl, 5 mM EDTA, 50 mM sodium fluoride, 2 mM dithiothreitol, 0.25% Nonidet P-40, 1 mM phenylmethyl-sulfonyl fluoride, 10 μg/mL aprotinin, 10 μg/mL leupeptin and 1 μg/mL pepstatin A). The lysate was cleared by centrifugation and the protein concentration of the whole cell extract was measured using Bio-Rad DC protein assay kit (Bio-Rad). Equal amounts of cell lysates (10 μg protein) were resolved by 10% SDS-PAGE and transferred on nitrocellulose membrane followed by incubating with individual antibodies. The immumoreactive proteins were visualized by ECL (Asamitsu *et al.* 2003).

Determination of mitochondrial ΔΨm in cultured cells

To visualize the cells with depressed ΔΨm, cells growing on Laboratory-TekII chambered cover glass were stained with 40 nM CMX-Ros in PBS for 15 min, washed with PBS three times and observed under the confocal microscope (Bio-Rad MRC600UVF). The acquisitions of the mitochondrial images were provided by 585LP emission filter with same setting (Iris: 2.0, Gain: 1.4).

Cell survival assay

To quantitatively measure the cell survival, cell cultures were stained with trypan blue and counted under microscopy in triplicates. To

determine the anti-apoptotic effect of NF-κB, 293/53BP2 cells were cultured without pon A to 50% confluence, stimulated with pon A (5 μM), and after 24 h in culture they were treated with IL-1β (20 ng/mL). The cell survival was assessed every 24 h for an additional 4 days after the stimulation with IL-1β.

Electrophoretic mobility shift assay (EMSA)

293/53BP2 cells were pretreated with or without IL-1β (20 ng/mL) and nuclear extracts were prepared as previously described (Takada *et al.* 2002). The double-stranded oligonucleotide probe for NF-κB was synthesized and end-labeled by γ-[^{32}P]-dATP. The κB sequence was taken from the human immunodeficiency virus long-terminal repeat (HIV-LTR). The κB sequence used was forward (5′-TTT CTA GGG ACT TTC CGC CTG GGG ACT TTC CAG-3′) and complement (5′-TTT CTG GAA AGT CCC CAG GCG GAA AGT CCC TAG-3′). Nuclear extracts were incubated in 10 μL EMSA buffer containing the radiolabelled κB oligonucleotide probe. The samples were analyzed by 6% non-denaturing PAGE. For NF-κB supershift assay, antibodies to NF-κB p65 and/or p50 subunits were added (30 min, 4 °C).

Acknowledgements

We thank Dr. Louie Naumovski (Stanford University) for the generous gifts of 293/53BP2 cells and polyclonal antibody to 53BP2S/Bbp. This work was supported in part by Grants-in-Aid from the Ministry of Health, Labor and Welfare, and the Ministry of Education, Culture, Sports, Science and Technology of Japan, and Japanese Human Sciences Foundation.

References

Ao, Y., Rohde, L.H. & Naumovski, L. (2001) p53-interacting protein 53BP2 inhibitsclonogenic survival and sensitizes cells to doxorubicin but not paclitaxel-induced apoptosis. *Oncogene* **20**, 2720–2725.

Arlt, A., Vorndamm, J., Müerköster, S., *et al.* (2002) Autocrine production of interleukin 1beta confers constitutive nuclear factor κB activity and chemoresistance in pancreatic carcinoma cell lines. *Cancer Res.* **62**, 910–916.

Asamitsu, K., Kanazawa, S., Tetsuka, T. & Okamoto, T. (2003) RING finger protein AO7 supports NF-kappaB-mediated transcription by interacting with the transactivation domain of the p65 subunit. *J. Biol. Chem.* **278**, 26879–26887.

Bergamaschi, D., Samuels, Y., Jin, B., Duraisingham, S., Crook, T. & Lu, X. (2004) ASPP1 and ASPP2: common activators of p53 family members. *Mol. Cell. Biol.* **24**, 1341–1350.

Bottero, V., Rossi, F., Samson, M., Mari, M., Hofman, P. & Peyron, J.F. (2001) IκBα, the NF-κB inhibitory subunit, interacts with ANT, the mitochondrial ATP/ADP translocator. *J. Biol. Chem.* **276**, 21317–21324.

Chen, C., Edelstein, L.C. & Gelinas, C. (2000) The Rel/NF-κB family directly activates expression of the apoptosis inhibitor Bcl-X_L. *Mol. Cell. Biol.* **20**, 2687–2695.

Chen, F., Castranova, V. & Shi, X. (2001) New insights into the role of nuclear factor-κB in cell growth regulation. *Am. J. Pathol.* **159**, 387–397.

Chu, Z.L., McKinsey, T.A., Liu, L., Gentry, J.J., Malim, M.H. & Ballard, D.W. (1997) Suppression of tumor necrosis factor-induced cell death by inhibitor of apoptosis c-IAP2 is under NF-κB control. *Proc. Natl. Acad. Sci. USA* **94**, 10057–10062.

Cogswell, P.C., Kashatus, D.F., Keifer, J.A., *et al.* (2003) NF-κB and IκBα are found in the mitochondria. Evidence for regulation of mitochondrial gene expression by NF-κB. *J. Biol. Chem.* **278**, 2963–2968.

Daniel, N.N. & Korsmeyer, S.J. (2004) Cell death: critical control points. *Cell* **116**, 205–219.

DeLuca, C., Kwon, H., Pelletier, N., Wainberg, M.A. & Hiscott, J. (1998) NF-κB protects HIV-1-infected Myeloid cells from apoptosis. *Virology* **244**, 27–38.

Gorina, S. & Pavletich, N.P. (1996) Structure of the p53 tumor suppressor bound to the ankyrin and SH3 domains of 53BP2. *Science* **274**, 1001–1005.

Haddad, J.J. (2004) On the antioxidation mechanisms of Bcl-2: a retrospective of NF-κB signaling and oxidative stress. *Biochem. Biophys. Res. Commun.* **322**, 355–363.

Iwabuchi, K., Bartel, P.L., Li, B., Marraccino, R. & Fields, S. (1994) Two cellular proteins that bind to wild-type but not mutant p53. *Proc. Natl. Acad. Sci. USA* **91**, 6098–6102.

Iwabuchi, K., Li, B., Massa, H.F., Trask, B.J., Date, T. & Fields, S. (1998) Stimulation of p53-meditated transcriptional activation by the p53-binding proteins, 53BP1 and 53BP2. *J. Biol. Chem.* **273**, 26061–26068.

Kajino, S., Suganuma, M., Teranishi, F., *et al.* (2000) Evidence that de novo protein synthesis is dispensable for anti-apoptotic effects of NF-κB. *Oncogene* **19**, 2233–2239.

Karin, M. & Lin, A. (2002) NF-κB at the crossroads of like and death. *Nature Immunol.* **3**, 221–227.

Kobayashi, S., Kajino, S., Takahashi, N., *et al.* (2005) 53BP2 induces apoptosis through the mitochondrial death pathway. *Genes Cells* **3**, 253–260.

Lopez, C.D., Ao, Y., Rohde, L.H., *et al.* (2000) Proapoptotic p53-interacting protein 53BP2 is induced by UV irradiation but suppressed by p53. *Mol. Cell. Biol.* **20**, 8018–8025.

Mori, T., Okamoto, H., Takahashi, N., Ueda, R. & Okamoto, T. (2000) Aberrant overexpression of 53BP2 mRNA in lung cancer cell lines. *FEBS Lett.* **465**, 124–128.

Naumovski, L. & Cleary, M.L. (1996) The p53-binding protein 53BP2 also interacts with Bc12 and impedes cell cycle progression at G2/M. *Mol. Cell. Biol.* **16**, 3884–3892.

Samuels-Lev, Y., O'Connor, D.J., Bergamaschi, D., *et al.* (2001) ASPP proteins specifically stimulate the apoptotic function of p53. *Mol. Cell* **8**, 781–794.

Shimizu, S., Eguchi, Y., Kamiike, W., *et al.* (1996) Bcl-2 blocks loss of mitochondrial membrane potential while ICE inhibitors act at a different step during inhibition of death induced by respiratory chain inhibitors. *Oncogene* **13**, 21–29.

Shimizu, S., Konishi, A., Kodama, T. & Tsujimoto, Y. (2000) BH4 domain of antiapoptotic Bcl-2 family members closes voltage-dependent anion channel and inhibits apoptotic

mitochondrial changes and cell death. *Proc. Natl. Acad. Sci. USA* **97**, 3100–3105.

Takada, N., Sanda, T., Okamoto, H., *et al.* (2002) RelA-associated inhibitor blocks transcription of human immunodeficiency virus type1 by inhibiting NF-κB and Sp1 actions. *J. Virol.* **76**, 8019–8030.

Takahashi, N., Kobayashi, S., Jiang, X., *et al.* (2004) Expression of 53BP2 and ASPP2 proteins from TP53BP2 gene by alternative splicing. *Biochem. Biophys. Res. Commun.* **315**, 434–438.

Wu, M.X., Ao, Z., Prasad, K.V., Wu, R. & Schlossman, S.F. (1998) IEX-1L, an apoptosis inhibitor involved in NF-κB-mediated cell survival. *Science* **281**, 998–1001.

Yang, J.P., Ono, T., Sonta, S., Kawabe, T. & Okamoto, T. (1997) Assignment of p53 binding protein (TP53BP2) to human chromosome band 1q42.1 by in situ hybridization. *Cytogenet. Cell Genet.* **78**, 61–62.

Yang, J.P., Hori, M., Takahashi, N., Kawabe, T., Kato, H. & Okamoto, T. (1999) NF-κB subunit p65 binds to 53BP2 and inhibits cell death induced by 53BP2. *Oncogene* **18**, 5177–5186.

Yoshikawa, H., Nagashima, M., Khan, M.A., McMenamin, M.G., Hagiwara, K. & Harris, C.C. (1999) Mutational analysis of p73 and p53 in human cancer cell lines. *Oncogene* **18**, 3415–3421.

Received: 27 January 2005
Accepted: 05 May 2005

THE JOURNAL OF BIOLOGICAL CHEMISTRY
Vol. 280, No. 29, Issue of July 22, pp. 26701–26713, 2005
Printed in U.S.A.

Induction of *OGG1* Gene Expression by HIV-1 Tat*

Received for publication, March 25, 2005, and in revised form, June 1, 2005
Published, JBC Papers in Press, June 1, 2005, DOI 10.1074/jbc.M503313200

Kenichi Imai‡, Kenji Nakata‡, Kazuaki Kawai§, Takaichi Hamano¶, Nan Mei§, Hiroshi Kasai§, and Takashi Okamoto‡‖

From the ‡Department of Molecular and Cellular Biology, Nagoya City University Graduate School of Medical Sciences, 1 Kawasumi, Mizuho-cho, Mizuho-ku, Nagoya, Aichi 467-8601, the §Department of Environmental Oncology, Institute of Industrial Ecological Sciences, University of Occupational and Environmental Health, Kitakyushu, Fukuoka 807-8555, and the ¶AIDS Research Center, National Institute of Infectious Diseases, 1-23-1 Toyama, Shinjuku-ku, Tokyo 162-8640, Japan

To identify the cellular gene target for Tat, we performed gene expression profile analysis and found that Tat up-regulates the expression of the *OGG1* (8-oxoguanine-DNA glycosylase-1) gene, which encodes an enzyme responsible for repairing the oxidatively damaged guanosine, 8-oxo-7,8-dihydro-2′-deoxyguanosine (8-oxo-dG). We observed that Tat induced *OGG1* gene expression by enhancing its promoter activity without changing its mRNA stability. We found that the upstream AP-4 site within the *OGG1* promoter is responsible and that Tat interacted with AP-4 and removed AP-4 from the *OGG1* promoter by *in vivo* chromatin immunoprecipitation assay. Thus, Tat appears to activate *OGG1* expression by sequestrating AP-4. Interestingly, although Tat induces oxidative stress known to generate 8-oxo-dG, which causes the G:C to T:A transversion, we observed that the amount of 8-oxo-dG was reduced by Tat. When *OGG1* was knocked down by small interfering RNA, Tat increased the amount of 8-oxo-dG, thus confirming the role of OGG1 in preventing the formation of 8-oxo-dG. These findings collectively indicate the possibility that Tat may play a role in maintenance of the genetic integrity of the proviral and host cellular genomes by up-regulating OGG1 as a feed-forward mechanism.

Tat is an essential transactivator of human immunodeficiency virus (HIV)[1] gene expression and viral replication (1). Tat stimulates viral gene expression by directly binding to the characteristic RNA stem-loop-bulge structure called the transactivation response region located within the long terminal repeat (2, 3) and enhancing the processivity of RNA polymerase II (4, 5). The transcriptional activity of Tat is supported by interaction with cellular factors such as positive transcription elongation factor-b (6–8) and histone acetyltransferase (9). Cyclin T1, a regulatory subunit of the positive transcription elongation factor-b complex, binds to the activation domain of Tat and facilitates the hyperphosphorylation of the C-terminal domain of RNA polymerase II at the vicinity of HIV genes. Thus, Tat makes RNA polymerase II highly competent for the transcription elongation and productive expression of HIV genes (10).

Although much of the efforts in Tat studies have focused on its transcriptional activation from the HIV provirus, the actions of Tat on cellular genes have also been revealed. For example, Tat is known to promote cellular transformation (11), to induce oxidative stress (12, 13), and to elicit inflammatory reactions (14, 15). Choi *et al.* (16) observed that Tat transgenic mice exhibit decreased gene expression of the γ-glutamylcysteine synthetase regulatory subunit and decreased GSH content in tissues. These biological actions of Tat are considered to cause activation of nuclear factor-κB, AP-1 (activating protein-1), and mitogen-activated protein kinase (13, 17). These findings prompted us to search for cellular target genes of Tat, either up-regulated or down-regulated, using a gene expression profile analysis.

In addition to the very high efficiency of the viral replication rate that is mainly ascribable to Tat action, HIV owes its morbidity to its high mutation rate, leading to the emergence of drug resistance and escape from the host immune response. In fact, the high frequency of G:C to A:T and G:C to T:A mutations was previously observed in HIV-1 and other lentiviruses (18–21). Recent studies (22–25) have deciphered one such mechanism that involves the HIV-encoded virion infectivity factor blocking the enzymatic activity of cytidine deaminase CEM15 (also known as APOBEC3G for apolipoprotein B mRNA-editing enzyme, catalytic polypeptide-like 3G), which induces G:C to A:T hypermutation in newly synthesized DNA. Another type of mutation, G:C to T:A transversion, is mediated by the generation of 8-oxo-7,8-dihydro-2′-deoxyguanosine (8-oxo-dG) by radical oxygen species (ROS) and occurs at the DNA level (26, 27). The oxidatively damaged guanosine, 8-oxo-dG, is widely accepted as a pre-mutagenic lesion because of its potential to mispair with adenine, thus generating the G:C to T:A transversion. This type of mutation is often found in tumor suppressor genes and oncogenes, such as p53 and K-*ras*, in mammalian cells (28, 29). The OGG1 (8-oxoguanine-DNA glycosylase-1) enzyme is responsible for the excision/repair of this oxidatively damaged DNA by excising 8-oxo-dG (30–32). In fact, *OGG1* gene knockout actually shows accumulation of such a mutation (33, 34).

In this study, we demonstrate the up-regulation of OGG1 by Tat and provide evidence that this effect of Tat is through the sequestration of the negative transcription factor AP-4 for the expression of *OGG1*. We examine the effect of Tat on the actual

* This work was supported in part by grants-in-aid from the Ministry of Health, Labor, and Welfare of Japan, the Ministry of Education, Culture, Sports, Science, and Technology of Japan, and the Japanese Health Sciences Foundation. The costs of publication of this article were defrayed in part by the payment of page charges. This article must therefore be hereby marked "*advertisement*" in accordance with 18 U.S.C. Section 1734 solely to indicate this fact.

‖ To whom correspondence should be addressed. Tel.: 81-52-853-8204; Fax: 81-52-859-1235; E-mail: tokamoto@med.nagoya-cu.ac.jp.

[1] The abbreviations used are: HIV, human immunodeficiency virus; 8-oxo-dG, 8-oxo-7,8-dihydro-2′-deoxyguanosine; ROS, radical oxygen species; siRNA, small interfering RNA; mTat, mutant Tat; PonA, ponasterone A; PBMCs, peripheral blood mononuclear cells; RT, reverse transcription; PBS, phosphate-buffered saline; ChIP, chromatin immunoprecipitation; HPLC, high performance liquid chromatography; ECD, electrochemical detector.

levels of 8-oxo-dG in the presence and absence of small interfering RNA (siRNA) against *OGG1* mRNA.

EXPERIMENTAL PROCEDURES

Plasmids—The cDNA of wild-type Tat (101 amino acids) originating from HIV-1 was amplified by PCR with the oligonucleotide primer pair 5′-CGC GGA TCC GCG CCA CCA TGG ATT ACA AGG ATG ACG ACG ATA AGA TGG AGC CAG TAG ATC CTA GAC TAG AGC CCT GG-3′ (forward; containing an EcoRI site and a FLAG epitope) and 5′-CCG GAA TTC CGG CTG ATG GAC CGG ATC TGT CTC-3′ (reverse; containing a BamHI site). The amplified DNA fragment was digested with EcoRI and BamHI and ligated in-frame into the pIND-V5 expression vector (Invitrogen), thus generating pIND-Tat. As a control, we employed mutant Tat (mTat) lacking transcriptional activity because of the absence of binding activity with cyclin T1 or the transactivation response region (6–8). The plasmid expressing mutant Tat (pIND-mTat) in which Cys^{30} and Lys^{41} were substituted with Ala was generated using a QuikChange site-directed mutagenesis kit (Stratagene) with the following mutagenic oligonucleotide primer pairs: 5′-CTA TTG TAA AAA GGC CTG CTT TCA TTG CC-3′ (forward) and 5′-GGC AAT GAA AGC AGG CCT TTT TAC AAT AG-3′ (reverse) or 5′-GTT TCA CAA CAG CCG CCT TAG GCA TC-3′ (forward) and 5′-GAT GCC TAA GGC GGC TGT TGT GAA AC-3′ (reverse). To generate the mammalian expression plasmid for AP-4, AP-4 gene was amplified by PCR with the oligonucleotide primer pair 5′-CGC GGA TCC GCG CCA CCA TGG ATT ACA AGG ATG ACG ACG ATA AGA TGG AGC CAG TAG ATC CTA GAC TAG AGC CCT GG-3′ (forward; containing an EcoRI site) and 5′-CCG GAA TTC CGG CTG ATG GAC CGG ATC TGT CTC-3′ (reverse; containing a BamHI site). The amplified DNA fragment was digested with EcoRI and BamHI and ligated in-frame into the pcDNA-Myc expression vector (Invitrogen). The construction of pCD12-luc, containing the HIV-1 long terminal repeats V3 and R linked to the luciferase gene, and pcDNA-Tat was described previously (35, 36). Human *OGG1* promoter-luciferase fusion constructs, including pPR116, pPR128, pPR130, and pPR143, were kindly provided by Dr. J. P. Radicella (Radiobiologie Moleculaire et Cellulaire, CNRS-CEA, Fontenay aux Roses, France) (37). The mutant pPR128-luc reporter constructs were generated using a QuikChange site-directed mutagenesis kit. The mutant sequences (sense strand) utilized were as follows: 5′-AP-4 site mutant (m5′AP-4), GAC GGC AGG CAG tcg cga TGG CGG CCG GCG; 3′-AP-4 site mutant (m3′AP-4), GGG AAA GGC GAG tcg cga GCA GAG AGC CCA G; GA TA site mutant (mGATA), CTT GCA GCC Tct TAG TTA AGA TAC AGC; and AP-2 site mutant (mAP-2), CAG CTG TGG CGG CCa ttC GGG ACG ACA ATC (with consensus binding sites underlined and mutated sequences in lowercase letters). The construct containing mutations in both the 5′- and 3′-AP-4 sites (mwAP-4) was generated by two successive PCRs using the m5′AP-4 and m3′AP-4 mutant sequences. The control luciferase reporter plasmid pGL3-Basic vector was purchased from Promega. All constructs were confirmed by dideoxynucleotide sequencing using an ABI PRISM™ dye terminator cycle sequencing ready kit (PerkinElmer Life Sciences) on an Applied Biosystems 313 Automated DNA Sequencer.

Cell Lines That Inducibly Express Tat, mTat, and LacZ—HEK293-EcR cells, stably transfected with pVgRXR expressing the ecdysone receptor, were purchased from Invitrogen and transfected with pIND-Tat and pIND-mTat to establish Tat/293 and mTat/293 cells, respectively. The control cell line (LacZ/293) was a gift from Dr. L. Naumovski (Stanford University, Stanford, CA) (38). Expression of these genes is under the stringent control of a homolog of the insect hormone 20-OH-ecdysone, ponasterone A (PonA; Invitrogen). Cells containing these plasmids were selected by 500 μg/ml G418 and 450 μg/ml Zeocin. Cell clones were singly isolated by two successive rounds of limiting dilution of cells and were screened for the expression and transcriptional activity of Tat proteins.

Cell Culture—Tat/293, mTat/293, and LacZ/293 cells were grown at 37 °C in Dulbecco's modified Eagle's medium (Sigma) with 10% heat-inactivated fetal bovine serum (Immuno-Biological Laboratories, Maebashi, Japan), 100 units/ml penicillin, and 100 μg/ml streptomycin. The Jurkat T cell line was maintained in RPMI 1640 medium (Sigma) with 10% fetal bovine serum, penicillin, and streptomycin. Peripheral blood mononuclear cells (PBMCs) were isolated from healthy donors, stimulated with phytohemagglutinin for 48 h, and further cultured in RPMI 1640 medium supplemented with 10% heat-inactivated fetal bovine serum and 20 units/ml interleukin-2.

Preparation of mRNA—Total cellular RNA was prepared from each cell clone using RNeasy (Qiagen Inc.). Purification of polyadenylated mRNA was carried out using an Oligotex-dT30 super RNA purification kit (Takara, Ohtsu, Japan) as described previously (39, 40). The mRNA samples were digested with RNase-free DNase, ethanol-precipitated, and further purified through Microcon YM-100 columns (Amicon Inc.). The quantity and quality of mRNA were assessed by capillary electrophoresis using an Agilent 2100 bioanalyzer.

Generation of Fluorescently Tagged cDNA and Gene Expression Profile Analysis—Gene expression profiles were examined as described (39, 40) using the human 3K DNA CHIP™ (Takara) containing 2600 human genes of known functions. Briefly, fluorescently labeled cDNA was synthesized from 1-μg aliquots of purified mRNA by oligo(dT)-primed polymerization using SuperScript II reverse transcriptase (Invitrogen). The pool of nucleotides in the labeling reaction contained 0.5 mM each dGTP, dATP, and dTTP; 0.3 mM dCTP; and 0.1 mM fluorescent nucleotide (Cy3- or Cy5-labeled dCTP, Amersham Biosciences). Fluorescently labeled cDNA was purified by chromatography through Microcon YM-20 columns (Amicon Inc.). The microarray slide was hybridized to combined Cy5-dCTP- and Cy3-dCTP-labeled cDNA probes for 14 h in hybridization solution (6× SSC and 0.2% SDS with 5× Denhardt's solution and carrier DNA) at 65 °C under coverslips. After hybridization, the microarray slide was washed twice with 1.2× SSC and 0.2% SDS at 55 °C for 5 min, with 1.2× SSC and 0.2% SDS at 65 °C for 5 min, and with 0.05× SSC at room temperature as a final wash. The hybridized array was scanned at 10-μm resolution on an Affymetrix 428 array scanner. Analysis of differential expression of each gene was performed using ImaGene Version 4.2 computer software (Bio-Discovery Ltd.). Normalization of hybridized signals was performed by global scaling. These experiments were repeatedly performed: we performed comparative microarray analyses three times (24 h after PonA stimulation in 293/Tat and 293/LacZ cells) and two times (12 h after PonA stimulation in 293/Tat and 293/LacZ cells).

Co-immunoprecipitation and Immunoblot Assay—The experimental procedures have been described previously (41). Briefly, cells were harvested with lysis buffer (25 mM HEPES-NaOH (pH 7.9), 150 mM NaCl, 1.5 mM $MgCl_2$, 0.2 mM EDTA, 0.3% Nonidet P-40, 1 mM dithiothreitol, and 0.5 mM phenylmethylsulfonyl fluoride). The lysates were cleared by centrifugation, and the supernatants were incubated overnight with the indicated antibodies at 4 °C. For immunoprecipitation with the FLAG epitope, anti-FLAG antibody M2 affinity gel beads (Sigma) were used. The immune complexes were washed three times with 1 ml of lysis buffer, and the antibody-bound proteins were dissolved by boiling in 2× Laemmli sample buffer. After centrifugation, the supernatant proteins were separated by SDS-PAGE and transferred to nitrocellulose membrane (Hybond-C, Amersham Biosciences). The membrane was probed with antibodies, including anti-cyclin T1 and anti-AP-4 (Santa Cruz Biotechnology Inc.), anti-FLAG (Sigma), and anti-Myc (Invitrogen) antibodies; and immunoreactive proteins were visualized by enhanced chemiluminescence (SuperSignal, Pierce). To evaluate the level of OGG1 protein, cells were similarly treated with lysis buffer, and the cell lysate was analyzed by Western blotting using anti-OGG1 antibody (Novus Biologicals, Inc.).

Transfection and Luciferase Assay—Cells were transfected using FuGENE 6 transfection reagent (Roche Applied Science) as described (36). Jurkat cells were transiently transfected by electroporation (42). Briefly, cells (2×10^7/ml) were electroporated in the presence of 2 μg of pcDNA-Tat or control plasmid (pcDNA3.0, Invitrogen) in 400 μl of serum-free RPMI 1640 medium using the Electro Cell Manipulator 600 apparatus (BTX) at 260 V/1050 microfarads. For the internal control, we employed pRL-TK, expressing *Renilla* luciferase, which is not modified by Tat action. The transfected cells were harvested, and the extracts were subjected to luciferase assay using the Luciferase Assay System™ (Promega). The luciferase activity was normalized to *Renilla* luciferase activity as an internal control to assess the transfection efficiency. The data are presented as the -fold increase in luciferase activities (means ± S.D.) relative to the control from three independent transfections.

Reverse Transcription (RT)-PCR—For cDNA synthesis, 1 μg of purified total RNA were reverse-transcribed using oligo(dT) primer and SuperScript II reverse transcriptase. The cDNA was then amplified from each RNA sample with *Taq* PCR Master Mix (Qiagen Inc.) and gene-specific primers designed using Oligo Version 4.0 software (Molecular Biology Insights). The primer sequences for each amplified gene were as follows: *TFPI2* (tissue factor pathway inhibitor-2), 5′-CAG GAG CCA ACA GGA AAT AAC-3′ (forward) and 5′-GAA TAC GAC CCC AAG AAA TGA-3′ (reverse); *OGG1*, 5′-GCG TGC GCA AGT ACT TCC AGC-3′ (forward) and 5′-CCA GTG ATG CGG GCG ATG TTG-3′ (reverse); *OGG1* type 1, 5′-GCG TGC GCA AGT ACT TCC AGC-3′ (forward) and 5′-TAA AGG GAA GAT AAA ACC ATC-3′ (reverse); *OGG1* type 2, 5′-GCG TGC GCA AGT ACT TCC AGC-3′ (forward) and 5′-GCA TCA CAT GAC CAA TTA CTG-3′ (reverse); *MEN1β2* homolog